
Electronic Thesis and Dissertation Repository

8-20-2020 1:00 PM

Studies on Carbon Quantum Dots with Special Luminescent Properties and Their Capability of Overcoming the Biological Barriers

Ji Su Song, *The University of Western Ontario*

Supervisor: Zhang, Jin, *The University of Western Ontario*

A thesis submitted in partial fulfillment of the requirements for the Master of Engineering Science degree in Biomedical Engineering

© Ji Su Song 2020

Follow this and additional works at: <https://ir.lib.uwo.ca/etd>

Recommended Citation

Song, Ji Su, "Studies on Carbon Quantum Dots with Special Luminescent Properties and Their Capability of Overcoming the Biological Barriers" (2020). *Electronic Thesis and Dissertation Repository*. 7269.
<https://ir.lib.uwo.ca/etd/7269>

This Dissertation/Thesis is brought to you for free and open access by Scholarship@Western. It has been accepted for inclusion in Electronic Thesis and Dissertation Repository by an authorized administrator of Scholarship@Western. For more information, please contact wlsadmin@uwo.ca.

Abstract

Carbon dot (CD) is a recently discovered fluorescent nanoparticle that exhibits excellent optical properties while also displaying great biocompatibility. This thesis examines two applications of CD: development of self-illuminating CD and investigation of the ability of CD in crossing biological barriers.

The self-illumination of CD is achieved through bioluminescence resonance energy transfer (BRET) from a bioluminescent protein, *Renilla* luciferase, to CD. The synthesis of self-illuminating CD consisted of using N'-(3-dimethylaminopropyl)-N-ethylcarbodiimide as coupler with 0.20 mg/mL to 0.80 mg/mL of CD and incubating with 2 μ M Rluc for 6.5 hours. The BRET efficiency increased with increasing CD concentration.

Bovine blood retina barrier (BRB), was used a biological barrier model. CD was incubated inside the eye after the removal of the vitreous. Preliminary data suggests that CD can cross the BRB as CD was found in the retinal neural layer of BRB as well as the choroid layer of BRB after treatment.

Keywords

Carbon dot, *Renilla* luciferase, bioluminescent protein, bioluminescence resonance energy transfer, biological barrier, blood retina barrier

Summary for Lay Audience

Carbon dot (CD) is a nano sized synthetic material that was recently discovered. Because CD can fluoresce brightly, it has been mostly used to substitute less bright traditional dyes in bioimaging. As CD was recently discovered, the potential applications of CD have not been investigated thoroughly. The thesis consists of two studies: development of self-illuminating carbon dot and investigation if CD can cross biological barriers.

Although CD can fluoresce brightly, the major downside is that an external light source has to excite CD for its fluorescence. The external light source can result in inaccuracy in results and damage to samples as the light is very powerful. Self-illumination was achieved by conjugating a bioluminescent protein, *Renilla* luciferase (Rluc), to CD. Rluc fluoresces when its substrate, coelenterazine, is present; the fluorescence from Rluc can excite CD so that it fluoresces. Such mechanism is referred to as bioluminescence resonance energy transfer (BRET). The study found that the synthesis of self-illuminating CD consists of a coupler, N'-(3-dimethylaminopropyl)-N-ethylcarbodiimide, to help with the conjugation, 0.2 mg/mL to 0.8 mg/mL of CD and incubating it with 2 μ M of Rluc for 6.5 hours. The BRET efficiency was found to increase with increasing CD concentrations. Self-illumination eliminates the disadvantages of external light source while maintaining the bright fluorescence of CD.

Biological barriers are physical barriers that exists to closely monitor what goes in and out of the most important parts of the body such as the brain and the eye; only extremely small or very specific materials can therefore enter and exit the biological barriers. Because it is easier to access intact eye structure compared to the brain, cow eyes were used to represent biological barriers. After incubating CD inside the eyes, both the retinal neural layer, the inside layer of the eye, and the choroid layer, the outside layer of the eye, had fluorescence after treatment, which suggests that CD might be able to cross BRB. With CD potentially crossing BRB, further studies can be done within the medical field to investigate and treat diseases that occur across the barriers.

Co-Authorship Statement

All chapters were written by Ji Su Song with contribution by Chao Lu in Chapter 3 regarding nanoparticles in drug delivery systems. Reviewing and editing was done throughout the thesis by Dr. Jin Zhang.

Acknowledgments

First, I would like to express my greatest gratitude to my supervisor, Dr. Jin Zhang, who has supported me throughout my entire master's program from the beginning until the end. She has always offered guidance and advice throughout my projects to ensure that I was on the right track. I would not have been able to successfully complete my projects without her help and encouragement.

Second, I would like to extend my gratitude to the members of my advisory committee, Dr. Kathleen Hill and Dr. Amin Rizkalla. Their feedback and advice played a major role in the development of my project, and I greatly appreciate their help throughout the program.

Third, I would like to thank my lab mates: Songlin Yang, Eugene Hwang, Chao Lu, and Yingqi Zhang. Their support and contributions have greatly helped in my completion of the projects.

Finally, I would like to thank members of my personal life:

to my family, who has shown unconditional love and support throughout my educational carrier;

to my friends, Vicky Vo, Jessica Liu, Daphne Huang, Eunyoung Jeong, and Sana Nawab, who have always been there to emotionally support me and distract me with endless food dates;

to my partner, Gyeongsu Park, who has literally and figuratively lived through my undergraduate and graduate journey with me.

I do not think I would have been able to successfully complete my master's without the endless help and support I have gotten from everyone.

I would like to acknowledge the support from the Natural Sciences and Engineering Research Council of Canada (NSERC) and the Western Engineering Graduate Scholarship.

Table of Contents

Abstract	ii
Summary for Lay Audience	iii
Co-Authorship Statement	iv
Acknowledgments	v
Table of Contents	vi
List of Tables	ix
List of Figures	x
List of Abbreviations	xii
List of Appendices	xiv
Chapter 1	1
1 Introduction	1
1.1 Fluorescent Nanoparticles	1
1.2 Carbon Dots	2
1.2.1 Introduction	2
1.2.2 Synthesis of CD	2
1.2.3 Optical Properties of CD	3
1.2.4 Other Properties of CD	4
1.2.5 Applications of CD	5
1.3 Thesis Overview	6
Chapter 2	8
2 Literature Review	8
2.1 Literature Review for Chapter 3	8
2.1.1 Fluorescence Resonance Energy Transfer	8
2.1.2 Bioluminescent Proteins	11

2.2 Literature Review for Chapter 4	14
2.2.1 Biological Barriers	14
2.2.2 Mechanism of BBB transport	17
2.2.3 Nanoparticles in Crossing Biological Barriers	18
2.2.4 Nanoparticles in Drug Delivery to Biology Barriers	19
Chapter 3	21
3 Self-illumination of Carbon Dots by Bioluminescence Resonance Energy Transfer..	21
3.1 Introduction.....	21
3.2 Materials and Methods.....	23
3.2.1 Materials	23
3.2.2 Carbon Dot Synthesis	23
3.2.3 Bioconjugation of <i>Renilla</i> Luciferase with Carbon Dot	23
3.2.4 Photoluminescence Study	23
3.3 Results.....	24
3.3.1 Bioluminescence of <i>Renilla</i> Luciferase and Photoluminescence of Carbon Dot.....	24
3.3.2 The Factors on the Performance of BRET.....	27
3.4 Discussion	31
3.5 Conclusion	32
Chapter 4.....	33
4 Investigation of Carbon Dot Crossing Bovine Blood Retina Barrier	33
4.1 Introduction.....	33
4.2 Materials and Methods.....	33
4.2.1 Materials	33
4.2.2 Carbon Dot Synthesis	34
4.2.3 Preparation of Bovine Retina.....	34

4.2.4	Fluorescence Study	36
4.3	Results.....	36
4.3.1	Neural Retinal Layer.....	36
4.3.2	Choroid Layer	37
4.4	Discussion.....	38
4.5	Conclusion	38
Chapter 5	40
5	Summary and Future Work.....	40
5.1	Summary	40
5.2	Limitations and Future Work.....	41
5.2.1	Self-illuminating CD.....	41
5.2.2	CD crossing BRB.....	42
5.3	References.....	42
Appendices	54
Curriculum Vitae	57

List of Tables

Table 1: Summary of bioluminescent proteins.	12
---	----

List of Figures

Figure 1: Visual representation of the <i>Renilla</i> luciferase enzymatic reaction. Coelenterazine is the substrate. The enzymatic reaction results in a product, coelenteramide, but also a byproduct, blue light at 480 nm.	10
Figure 2: Different layers of the BRB. The two layers of BRB, choroid layer and neural retina layer, are pictured. Note that the sclera and the vitreous are not part of the BRB structure.....	16
Figure 3: EDC- or EDC/NHS-mediated conjugation of bioluminescent protein, Rluc to CDs. Both crosslinkers couple the free surface carboxylic acids on the CD with the amine group on the N-terminal of Rluc to form peptide bond. The close proximity between CD and Rluc after conjugation allows for BRET.	22
Figure 4: (a) Bioluminescence of 2.0 μ M Rluc reacting with 7.8 μ M CTZ. The small inset shows the purified Rluc on the SDS-PAGE gel. (b) Bioluminescence intensity as a function of the concentration of CTZ, its substrate.....	25
Figure 5: Photoluminescence of CDs under an excitation wavelength of 480 nm. TEM micrograph of CDs is shown in the small inset of the figure.....	26
Figure 6: Emission spectra of EDC- and EDC/NHS-mediated conjugation of Rluc and CD. The concentration of CD was fixed at 0.20 mg/mL, and the conjugation time was fixed at 6.5 hours.....	27
Figure 7: Emission spectra of samples using different concentrations of CDs. EDC was used as the coupling agent, and the conjugation time was fixed at 6.5 hours.	28
Figure 8: Emission spectra of samples produced using different conjugation times. The concentration of the CD was fixed at 0.20 mg/mL, and EDC was used as the coupling agent.	29
Figure 9: (a) BRET profile of sample made using EDC as coupling agent with 0.20 mg/mL of CD and 2 μ M Rluc for 6.5 hours of incubation. The black line represents the emission	

spectrum of the sample, or the BRET profile. The red and blue line, which represents Rluc and CD respectively, were obtained using multi-peak fitting software. The small inset is the photo of 2 μ M Rluc and CD-Rluc complex. (b) BRET efficiency as a function of CD concentration..... 30

Figure 10: (a) Back of the bovine eye before extraocular tissue removal. (b) Back of the bovine eye after extraocular tissue removal. (c) Front of the bovine eye before extraocular tissue removal. (d) Front of the bovine eye after extraocular tissue removal..... 35

Figure 11: Experimental eye cup. Extraocular tissues have been removed and, the anterior segment and the vitreous are removed in preparation for CD treatment. 35

Figure 12: Emission spectra of free CD (green), neural retinal layer before CD treatment (blue), and neural retinal layer after CD treatment (orange). CD treatment consisted of 1 mL of 1 mg/mL CD incubated for 1.5 hours inside the eye cup. 37

Figure 13: Emission spectra of free CD (green), choroid layer before CD treatment, (blue) and choroid layer after CD treatment (orange). CD treatment consisted of 1 mL of 1 mg/mL CD incubated for 1.5 hours inside the eye cup. 37

List of Abbreviations

AMD	Age-related macular degeneration
AMT	Adsorptive-mediated transcytosis
Au-NP	Gold nanoparticles
BBB	Blood-brain barrier
BRB	Blood-retina barrier
BRET	Bioluminescence resonance energy transfer
CD	Carbon dot
CMT	Carrier-mediated transport
CNS	Central nervous system
CRET	Chemical resonance energy transfer
CTZ	Coelenterazine
EDC	N'-(3-dimethylaminopropyl)-N-ethylcarbodiimide
FITC	Fluoresceinisothiocyanate
Fluc	Firefly luciferase
FMNH ₂	Flavin mononucleotides
FNP	Fluorescent nanoparticle
FRET	Fluorescence resonance energy transfer
Gluc	<i>Gaussia</i> luciferase
GLUT1	Glucose transporter type 1
HT-29	Human colorectal adenocarcinoma
iBRB	Inner blood-retina barrier
K _m	Michaelis constant

LAT1	Large neutral amino acid transporter type 1
Lux	Bacterial luciferase
MCF-7	Michigan Cancer Foundation-7
MUC1	Mucin 1
NGR-QD	NGR-conjugated polyethylene glycol-quantum dot
NHS	N-hydroxysuccinimide
Nluc	Nano luciferase
NP	Nanoparticle
oBRB	Outer blood-retina barrier
PBS	Phosphate buffered saline
PEG	Polyethylene glycol
PEI	poly(ethylenimine)
PL	Photoluminescence
PPI	poly(propylene imine)
QD	Quantum dot
Rluc	<i>Renilla</i> luciferase
RMT	Receptor-mediated transport
SDS-PAGE	Sodium dodecyl sulfate polyacrylamide gel electrophoresis
UV	Ultraviolet
Vluc	Vargula luciferase

List of Appendices

Appendix 1: UV-vis absorption spectrum of different concentrations of CDs.	54
Appendix 2: (a) BRET spectrum of sample made through EDC-mediated conjugation of 0.40 mg/mL CD and 2 μ M Rluc for 6.5 hours. (b) BRET spectrum of sample made through EDC-mediated conjugation of 0.80 mg/mL CD and 2 μ M Rluc for 6.5 hours. The black line represents the BRET profile of the sample; the red line and the blue line were obtained using multi-peak fitting and represent bioluminescence of Rluc and photoluminescence of CD respectively.	55
Appendix 3: Bioluminescence of Rluc as a function of time after introduction of CTZ.....	56

Chapter 1

1 Introduction

1.1 Fluorescent Nanoparticles

The world of nanoparticles (NP) is broad, as all particles within the nano scale size, a range of 10–1000 nm, are categorized as nanoparticles [1]. Out of these nanoparticles, some have been shown to have unique chemical and optical properties, which have led to the subcategorization of fluorescent nanoparticles (FNP).

After their discovery, FNPs have been used to substitute traditional organic dyes in fluorescence studies because they possess superior photostability, brighter fluorescence, and distinct size-dependency in fluorescence [2,3]. Although different technologies used in fluorescence studies have improved using different sensing modes with high sensitivities, the low absorption coefficients, short fluorescent lifetime, and weak signaling of organic dyes have been problematic in fluorescent studies [4]. Naturally, researchers were fast to substitute organic dyes with FNPs immediately following their discovery. Since then, different FNPs have been implemented in various fluorescence studies, from simple biolabeling to the development of fluorescent sensors [5–8].

Apart from these unique optical properties, FNPs are also useful as they have the potential to act as a scaffold for domain addition in target-specific studies [9,10]. With high surface-to-volume ratio, distinct spatial domains can be functionalized providing a high potential synthetic platform for different sensor systems [3]. The developments in the field of FNP have not only helped in fluorescent studies but have also opened a multitude of doors in the field of target-specific fluorescent studies, which are arguably more important within the biomedical field.

FNPs can be further categorized based on their synthesis material, such as metal NPs, quantum dots (QD), and carbon dots (CD). Out of the different types of FNPs, quantum dots and carbon dots are of special interest as their characteristics can be controlled by manipulating different steps during synthesis [3,11]. Because QDs have been developed

before CDs, there are more studies focusing on the synthesis and characterization of different QDs [12,13]. However, despite its superior brightness and wide excitation and emission spectra, the major downfall of QD is its biotoxicity. As the materials used to synthesize QD most often include heavy toxic metals, although QDs are small in size, their toxicity cannot be ignored in *in vivo* studies. Such drawbacks have led to a development of new synthetic FNPs that could exhibit the strong optical capabilities of QD while also being biocompatible.

1.2 Carbon Dots

1.2.1 Introduction

CDs are approximately spherical in shape with a diameter of less than 10 nm [14,15]. As the name indicates, CD core is primarily composed of carbon but other elements, such as nitrogen and oxygen, can also be present depending on the starting ingredient of CD. Unlike highly toxic QDs, CDs possess excellent biocompatibility as well as high water solubility, excellent optical properties, and potential for easy surface functionalization; moreover, in comparison to QD synthesis, CD synthesis is much simpler and more cost-effective. They are also more inert within the biological microenvironment, which allows for further research and development within the field [16]. Because of their superiority over QDs, CDs have been of interest in *in vivo* technologies, including bioimaging, biosensors, and drug delivery.

1.2.2 Synthesis of CD

1.2.2.1 Top-down synthesis

There are three different top-down methodologies for CD synthesis: laser ablation, arc discharge, and electrochemical approach. Only laser ablation will be discussed further as it is the most common and simplest form of CD top-down synthesis.

Laser ablation refers to a method in which laser irradiates a carbon target in order to produce a CD. A study by Sun and his colleagues demonstrate CD synthesis where the carbon target was a mixture of graphite powder and cement to obtain nano-sized carbon particles [17]. Although the resulting particles were not fluorescent, further treatment

with nitric acid with polyethylene glycol (PEG) resulted in 5 nm fluorescent CDs. Similarly, Hu and his colleagues used graphite flakes suspended in PEG solution as the carbon target to obtain CDs through laser ablation [18]. The resulting black solution was centrifuged to isolate the CDs, and the obtained CDs were shown to be fluorescent. It was also discovered that the size and microstructure of CDs could be controlled by manipulating pulse width of the millisecond-pulsed laser. Despite the simplicity of laser ablation, this synthetic approach is not efficient as it requires excess carbon target for CD synthesis; furthermore, the size of the CD is difficult to control, resulting in low product yield.

1.2.2.2 Bottom-up synthesis

There are various bottom-up methods for the synthesis of CDs: pyrolytic process, template method, microwave-assisted method, and chemical oxidation approach. Like laser ablation in top-down synthesis, the microwave-assisted method is arguably one of the simplest methods for CD synthesis overall and will be discussed further.

The microwave-assisted method is not only simple but also convenient and rapid, resulting in functional CDs within a few minutes and with reasonable yield. Guan and his colleagues describe a synthetic method using folic acid molecule as carbon and nitrogen sources [19]. In summary, folic acid was dissolved in diethylene glycol then microwaved to obtain a red-brown suspension, which was dialyzed to obtain functional CDs. Another synthetic method is described by Qu and his colleagues in which citric acid was used as the carbon source and urea was used as the nitrogen source [20]. The substances were dissolved in distilled water and then microwaved to obtain a brown liquid, which was further processed using a vacuum oven to isolate the resulting functional CDs. In both studies, the product yield and quantum yield of the resulting CDs were improved compared to laser ablation method.

1.2.3 Optical Properties of CD

Although the size of the CD has been shown to have an effect on the optical properties of the CD, the exact mechanism of CD fluorescence is still unknown. Different theories have been brought forth to explain the fluorescence, including quantum size effect,

degree of surface oxidation, and surface functional groups [21]. Nevertheless, the fluorescent property of CDs has been demonstrated in many different studies; furthermore, CDs absorbing and emitting at different wavelengths have been recorded in numerous experiments with researchers manipulating CD size to obtain CDs with different fluorescent properties [16]. Interestingly, CDs also show strong absorption in the ultraviolet (UV) region; however, similar to fluorescence, the peaking pattern has been shown to be highly dependent on the size of the CD.

It is important to note that due to the novelty of CDs, more studies must be done to further clarify the different properties of CDs. In particular, investigation of the mechanism of CD fluorescence should be focused on to improve optical performance of CDs in the future.

1.2.4 Other Properties of CD

1.2.4.1 Photostability

Photostability refers to the ability of fluorescent material to be stable during continuous excitation. In general, CDs have shown excellent photostability, which is especially important in bioimaging. Wei and his colleagues have determined their CD to have superior photostability compared to the traditional fluorescein isothiocyanate (FITC) dye, QD, and previously reported polymer NPs [22]. Similarly, Ge and his colleagues have also compared the photostability between CDs and FITC by observing fixed-cell images of CD or FITC labelled HeLa cells [23]. It has been reported that the fluorescence of the CD was still clearly detectable 120 minutes after laser irradiation, while the fluorescence of FITC was undetectable only 10 minutes after laser irradiation.

1.2.4.2 Cytotoxicity

The cytotoxicity, or rather the biocompatibility, of CDs has been of high interest as it directly tackles the major disadvantage of already commercially available QDs. A previous study by Liu and his colleagues have reported no significant toxic effects of CDs on Michigan Cancer Foundation-7 (MCF-7) and human colorectal adenocarcinoma (HT-29) cell models [24]. Both cell lines displayed signs of proliferation and viability

suggesting the biocompatibility of CD. Male CD-1 mice were used for *in vivo* investigations of CD biocompatibility. Certain functional indicators, including but not limited to alanine amino transferase (ALT) and uric acid (UA), were shown to be at similar levels when compared to control mice; furthermore, serum biochemistry assays suggested that high dosage CD did not result in significant toxic effects. Moreover, histopathological analyses also demonstrated that the organ structures of the CD-treated mice were normal and nearly identical to the control group mice.

1.2.5 Applications of CD

1.2.5.1 Bioimaging

CDs have been reported for use in both *in vitro* and *in vivo* bioimaging, as they are an ideal dye candidate due to their strong fluorescence and low cytotoxicity.

In *in vitro* settings, CDs have been shown to be gradually taken up by HeLa cells as well as MCF-7 cells. The translocation from the extracellular environment to the cytoplasm was shown to be dependent on the size of the CD as well as surface charge, chemistry, and temperature [25,26]. Previous studies have also shown that when CD is modified with ligands for membrane receptors, the modified CDs are much more readily taken up by different cell models [27].

Unlike *in vitro* studies, *in vivo* studies are much more sensitive, due to the fact that particle size, surface charge, low cytotoxicity and sufficient cell uptake are all important parameters in *in vivo* imaging [16]. A study by Yang and his colleagues reported that CDs continually emitted fluorescence when injected into mice; moreover, in general, subcutaneous injection led to slow diffusion and eventual accumulation in the liver, while intravenous injection led to excretion of the CD through urine [28]. These particles were shown to exhibit good biocompatibility and low cytotoxicity.

1.2.5.2 Biosensor

Because of the simplicity of surface modification and the benign property of CDs, they are also an ideal base for biosensor development.

Li and his colleagues were able to develop a DNA sensor using CDs to selectively detect nucleic acid [29]. The sensing DNA was absorbed onto the surface of the CD through π - π interaction, leading to fluorescence quenching of CD; however, once the sensing DNA hybridized with the target DNA, the π - π interaction between CD and sensing DNA was eliminated, thereby recovering CD fluorescence.

Similarly, protein sensors have been made by modifying the CD surface with specific antibodies. Ma and his colleagues developed a recombinant CD by modifying the surface with antibodies against mucin 1 (MUC1) and MUC1 aptamer [30]. Due to the sandwiching interaction between MUC1, MUC1 antibody, and MUC1 aptamer, this interaction led to CD aggregation, ultimately resulting in fluorescence quenching of CD. This protein sensor was found to be sensitive as well as cost efficient and convenient.

1.2.5.3 Drug Delivery

Various studies have discussed the different uses of CDs in drug delivery systems. A study by Jing and his colleagues used CDs as a contrast agent to monitor release of drug real time [31]. CDs have also been used as a targeting domain for drug delivery using surface modification of the CD with a specific ligand for targeting [32,33]. Finally, CDs have also been used as nanocarriers for gene delivery where the DNA can be condensed on the surface of the CD for delivery [34]. Upon uptake by the cell, the cell showed higher gene expression of the corresponding DNA.

1.3 Thesis Overview

The thesis is comprised of a literature review followed by two separate investigations and then a final conclusion to consolidate the two studies.

Chapter 2 focuses on the literature review. Background knowledge specific to each study is presented to introduce the two different investigations.

Chapter 3 focuses on the development of the self-illuminating CD. This is the first of the two separate investigations in this thesis.

Chapter 3 focuses on the examination of the ability of the CD to cross biological barriers. This is the second of the investigations in this thesis.

Chapter 4 consolidates the previous two chapters into one coherent conclusion; furthermore, limitations and future work for the two investigations are also discussed in this section.

Chapter 2

2 Literature Review

2.1 Literature Review for Chapter 3

2.1.1 Fluorescence Resonance Energy Transfer

Fluorescence resonance energy transfer (FRET) is a mechanism initiated by a high-power light source exciting a donor molecule. The excited molecule then loses some of its energy to heat while emitting the majority of excited energy as a photon. Due to the loss of energy to heat, the donor molecule emits a photon at a longer wavelength compared to the photon used to excite the donor molecule. This photon then excites the acceptor molecule where a similar phenomenon occurs, resulting in a photon being released at an even lower wavelength. Because FRET is a mechanism that uses resonance energy transfer, FRET is a distance-dependent mechanism where closer proximity of donor to acceptor results in better excitation of the acceptor molecule.

FRET has been widely used in studies involving protein-protein interactions [35–37]; however, many of them suffer from limitations originating from the high-power light source, such as tissue autofluorescence, photobleaching, photocytotoxicity, and tissue damage [38]. Therefore, its use is limited to *in vitro* studies where photocytotoxicity and tissue damage are not of concern. Furthermore, the high-power light source may also introduce tissue autofluorescence and photobleaching, which results in inaccuracy. While the problem of tissue autofluorescence can be solved by the development of new FRET pairs, which utilize emission and excitation wavelengths that are not common in biological settings, the still-standing limitations stemming from the high-power light source cannot be ignored.

In order to eliminate the high-power light source, different modifications have been made to the FRET mechanism; two mechanisms that have resulted from these modifications are chemical resonance energy transfer (CRET) and bioluminescence resonance energy transfer (BRET).

2.1.1.1 Chemical Resonance Energy Transfer

CRET is initiated with a chemiluminescence reaction, where an electronically excited molecule drops its electron to the ground state while releasing the energy as light energy, i.e. a photon. The photon produced from the reaction then acts as the donor photon that excites the acceptor molecule, which then emits a photon at a different wavelength when bringing down its excited electron to ground state.

While CRET is able to successfully occur without the high-power light source, it has its own limitations in a biological environment. The initial chemiluminescence reaction most often requires metallic ions or catalyst enzymes; moreover, cofactors may also be necessary for the reaction to take place. While such requirements are not troublesome in *in vitro* studies, they pose many limitations in *in vivo* studies. Metallic ions are mostly toxic and therefore have low biocompatibility. Catalyst enzymes and cofactors may have sufficient biocompatibility; however, the possibility of the molecules interacting and producing unwanted reactions in the biological microenvironment cannot be ignored.

2.1.1.2 Bioluminescence Resonance Energy Transfer

BRET obtains its donor photon from natural bioluminescent molecules found in fireflies, jellyfish, and other organisms. When the bioluminescent protein is exposed to its substrate, an enzymatic reaction is initiated. The protein acts as an enzyme, and while working on the substrate, it also produces a photon as a byproduct. An example of this enzymatic reaction, in which the *Renilla* luciferase (Rluc) is the bioluminescent protein and coelenterazine is the substrate, is visualized in Figure 1. This byproduct photon is used as the donor photon to excite the acceptor molecule, which in turn releases its own photon to escape the excited state.

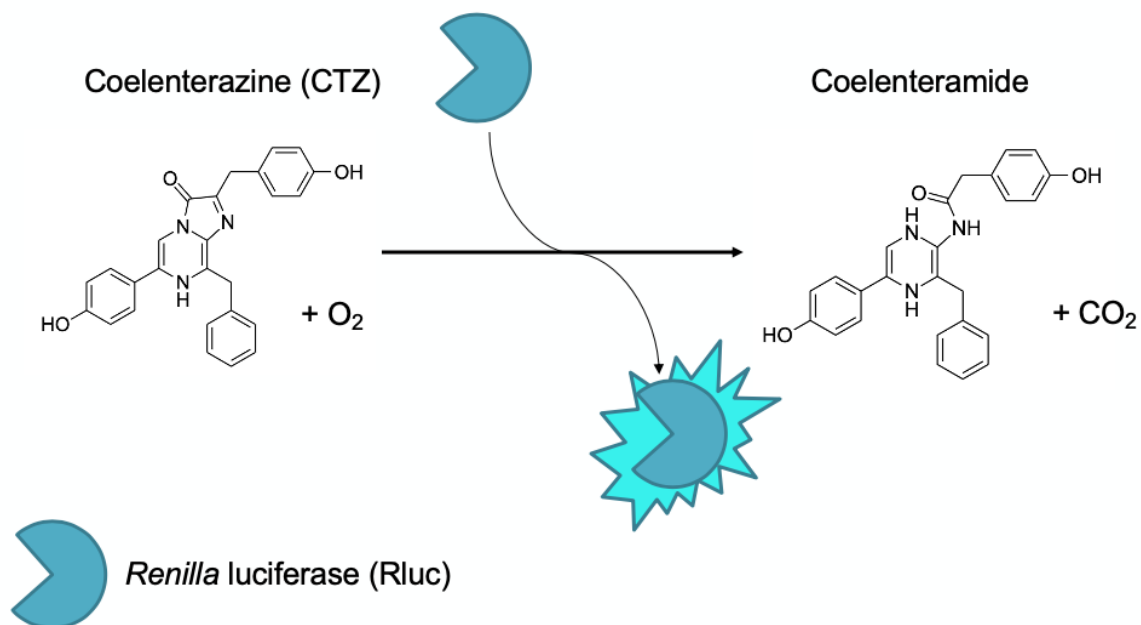


Figure 1: Visual representation of the *Renilla luciferase* enzymatic reaction. Coelenterazine is the substrate. The enzymatic reaction results in a product, coelenteramide, but also a byproduct, blue light at 480 nm.

As a derivative of FRET, BRET is highly distance-dependent: the donor molecule and acceptor molecule must be within 10 nm of one another for the energy transfer to occur. Also, because BRET derived from FRET, BRET is able to successfully substitute for FRET in previous studies that have utilized FRET. For example, in one previous study, a FRET dye-labeled probe was used to improve single-base mismatch discrimination in DNA detection [35]. Although this study was previously limited to *in vitro* study due to its need for external light source, such probe could be used in animal models if the FRET dye-labeled probe was BRET dye-labeled instead. As mentioned before, FRET has been used in many protein-protein interaction studies; therefore, the potential of BRET is just as widespread.

Unlike CRET, BRET only requires the bioluminescent protein and its appropriate substrate for the mechanism to initiate. Because the bioluminescent protein and its substrate are naturally occurring in specific organisms, they often have good biocompatibility with limited chance of unwanted interactions within the biological

microenvironment, as long as the *in vivo* study is completed using an organism that does not naturally use said molecules.

2.1.2 Bioluminescent Proteins

Bioluminescent proteins are naturally occurring enzymes in bioluminescent organisms, such as fireflies and sea pansies. More recent bioluminescent proteins were engineered in the laboratory setting to decrease the size of the protein for better biocompatibility while heightening its fluorescence intensity for more intense fluorescence signaling. Different bioluminescent proteins usually have different substrates required to complete their enzymatic reactions, and generally, the ideal bioluminescent protein and its substrate pair differs depending on the application and the biological microenvironment of the study.

Most known bioluminescent proteins fall under the luciferase family, which is a class of oxidative enzymes. The oxidation of luciferase results in an electron going from the excited state to its ground state while releasing the energy as a photon. This photon can then be used to excite other nearby molecules, as previously discussed.

A summary of different bioluminescent proteins is shown in Table 1.

Table 1: Summary of bioluminescent proteins.

Name	Size (kDa)	Emission (nm)	Substrate
Aequorin	22	469	Coelenterazine
Bacterial luciferase (Lux)	Alpha subunit: 40 Beta subunit: 35	490	FMNH ₂ , long-chain aliphatic aldehyde
Firefly luciferase (Fluc)	61	562	D-luciferin
<i>Renilla</i> luciferase (Rluc)	36	480	Coelenterazine
<i>Gaussia</i> luciferase (Gluc)	19.9	480	Coelenterazine
Vargular luciferase (Vluc) or <i>Cypridina</i> luciferase	62	460	Coelenterazine
<i>Metridia</i> luciferase	24	480	Coelenterazine
Nano luciferase (Nluc)	19	460	Furimazine

2.1.2.1 Aequorin

Aequorin is a 22 kDa photoprotein that is naturally occurring in jellyfish *Aequorea victoria*; it emits blue light at 469 nm as a byproduct of its enzymatic reaction, which uses coelenterazine as its substrate [39,40]. Aequorin is often used to detect calcium concentration due to its high sensitivity for calcium [41–43]. However, aequorin exhibits low light quantum yield in comparison to other bioluminescent proteins; furthermore, its substrate, coelenterazine, is unstable and has poor biodistribution [44].

2.1.2.2 Bacterial Luciferase

Bacterial luciferase (Lux) consists of two subunits: alpha and beta, which are 40 kDa and 35 kDa respectively [45]. Lux is an ATP-dependent luciferase and requires oxygen and NADPH as a cofactor in order for its enzymatic reaction to take place; long-chain

aliphatic aldehydes and flavin mononucleotides (FMNH₂) are its substrates, while the byproduct is blue light at 490 nm [46]. Like aequorin, Lux exhibits poor light quantum yield as well as poor thermostability [47]. Furthermore, studies with Lux are limited to luminous bacteria due to the cytotoxicity of the long-chain aliphatic aldehydes [48].

2.1.2.3 Firefly Luciferase

Firefly luciferase (Fluc) is a 61 kDa protein that is naturally occurring in fireflies; it emits blue light at 562 nm as a by-product after enzymatic reaction using D-luciferin [49,50].

Similar to Lux, Fluc is also ATP dependent and requires oxygen and magnesium as cofactors for its enzymatic reaction [50]. As the first luciferase to be discovered, Fluc has been extensively used in various studies across different fields; most notably, Fluc has been used to develop an ATP sensor, which takes advantage of the protein's ATP-dependency [51]. However, although Fluc exhibits higher light quantum yield in comparison to Lux and aequorin, D-luciferin does not display good biodistribution and has low affinity for Fluc [44]. As well, the large size of Fluc has been shown to lead to steric hindrance when developing recombinant proteins [52].

2.1.2.4 *Renilla* Luciferase

Renilla luciferase (Rluc) is a 36 kDa bioluminescent protein that is naturally occurring in the sea pansy, *Renialla reniformis*. Rluc uses coelenterazine (CTZ) as its substrate and generates blue luminescence at 480 nm, which falls within the excitation range of CDs. Because Rluc originates from a non-mammalian organism, certain codons used in Rluc expression are uncommon in mammalian cells, which limits Rluc expression in mammalian cells [53]. Rluc is well adapted in different scientific studies and has been used as marker for gene expression and a biosensor for certain proteins [54].

2.1.2.5 *Gaussia* Luciferase

Gaussia luciferase (Gluc) is a 19.9 kDa bioluminescent protein that originates from *Gaussia princeps*, a type of copepod [55]. Similar to Rluc, it also produces blue light at 480 nm and uses coelenterazine as its substrate. It has also been characterized to be more

sensitive compared to Fluc and Rluc; however, despite its the heightened sensitivity, the light quantum yield is low [44,56].

2.1.2.6 Vargula Luciferase

Vargula luciferase (Vluc), also known as *Cypridina* luciferase, is a 62 kDa protein that is naturally secreted by a marine ostracod, *Cypridina noctiluca* [57,58]. It emits blue light at 460 nm as a by-product of its enzymatic reaction with vargulin, also known as *cypridina* luciferin [58]. Like Rluc, Vluc has been previously used as a marker for mammalian gene expression, as well as a recombinant biosensor [58]. One advantage Vluc has over other bioluminescent proteins is its glow-type bioluminescence compared to others' flash-type bioluminescence [57].

2.1.2.7 Metridia Luciferase

Metridia luciferase is a 24 kDa protein that uses coelenterazine as its substrate and produces blue light at 480 nm similar to Rluc and Gluc [59,60]. Its low molecular mass is an advantage in the development of recombinant proteins; however, its low light quantum yield is a major disadvantage [59,59].

2.1.2.8 Nano Luciferase

Nano luciferase (Nluc) is one of the smallest luciferases at 19 kDa and was synthetically developed in order to tackle different disadvantages of luciferases [61,62]. It uses a new substrate, furimazine, which exhibits lower background noise compared to coelenterazine, and emits blue light at 460 nm as by-product [52,61]. Not many studies have been conducted using Nluc as the molecule was recently developed. Nluc exhibits glow-type bioluminescence with a long half-life of 2 hours [62].

2.2 Literature Review for Chapter 4

2.2.1 Biological Barriers

2.2.1.1 Blood Brain Barrier

The blood-brain barrier (BBB) is a physical barrier that maintains homeostasis within the central nervous system (CNS) by protecting it from toxins and metabolic fluctuations. It

is comprised mainly of endothelial cells with other supporting structures, such as brain capillaries, pericytes, astrocytes, and the basement membrane [63–67]. These structures work together to supply the brain with required nutrients, such as glucose and oxygen, for normal neural functioning, while preventing neurotoxins from entering the neural cavity. Because the brain is tightly packed with microvasculature, the neuronal cells are in close proximity to blood capillaries, which allows for fast delivery of substances once the BBB is crossed.

One of the differences between the capillaries of the BBB compared to capillaries found elsewhere in the body is the lack of fenestration in the endothelial cells [65]. The lack of fenestration prevents the passive diffusion of hydrophilic substances crossing the BBB through paracellular transport; furthermore, the endothelial cells are tightly packed and only connected through tight junctions, which helps in the prevention of paracellular transport [64–66]. Moreover, the electrical resistance of brain endothelium is much higher than other endothelial cells, which introduces even further limitations in paracellular transport. Due to these structural limitations, all substances cross the BBB via transcellular transport. There are few exceptions: very small (less than 400 Da), lipophilic molecules are able to diffuse through the lipid bilayer of the cell membrane [65].

Due to the complexity of the BBB structure, various drugs are blocked and cannot be delivered to the brain in sufficient quantity. This presents difficulties in treating CNS diseases, such as Parkinson's disease and Alzheimer's disease [63,64]. Drug delivery via intracerebral implantation and intracerebroventricular infusion have been attempted; however, such delivery methods present limitations in the dosage of the drug as well as a potential passage for infection [66,68]; moreover, they are also invasive procedures, which may lead to potentially detrimental side effects as well as low quality of life for patients. Thus, researchers and clinicians have focused on using the pre-existing transport mechanism of BBB to deliver drugs to the brain.

2.2.1.2 Blood Retina Barrier

Similar to the BBB, blood retina barrier (BRB) is also a physical barrier that exists to protect the retina. The BRB consist of inner BRB (iBRB) and outer BRB (oBRB). Figure 2 illustrates a diagram of different layers of the BRB. The oBRB consists of a retinal pigment epithelial (RPE) cell layer and regulates the movement of macromolecules from the choroid to the sub-retinal space. The iBRB is similar to the BBB and is comprised of retinal endothelial cells lining the microvasculatures to maintain the blood vessel and preserve homeostasis. Also similar to the BBB, both layers consists of tight junctions, which allow for the restriction of paracellular diffusion of molecules [69].

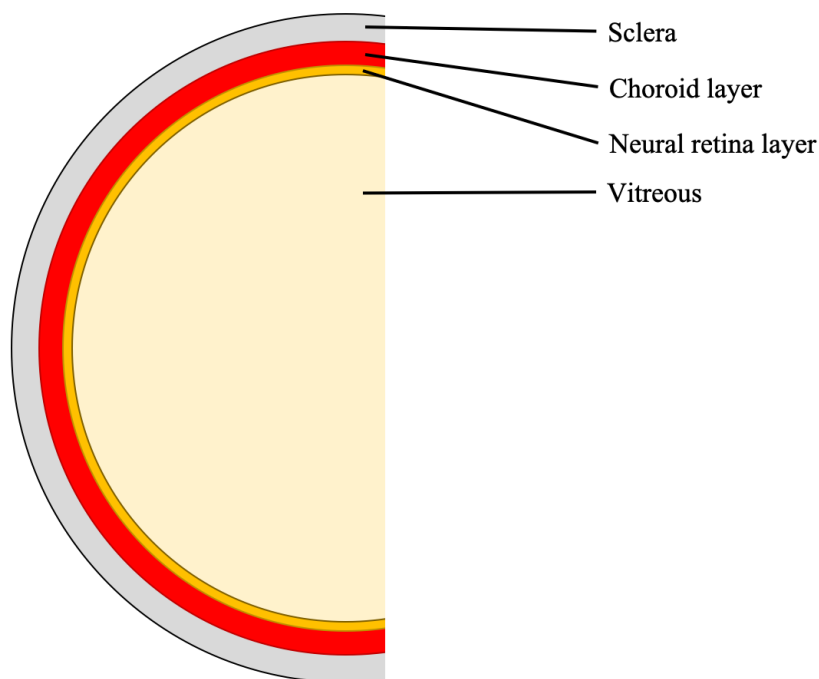


Figure 2: Different layers of the BRB. The two layers of BRB, choroid layer and neural retina layer, are pictured. Note that the sclera and the vitreous are not part of the BRB structure.

While damage to the BBB results in neurodegenerative diseases such as Alzheimer's, the breakdown of the BRB results in retinal diseases, such as age-related macular degeneration (AMD). Although antibody treatments are available for AMD, because of the selective nature of the BRB, treatments are given by direct intraocular injection into

the vitreous of the eye, which due to its invasive nature, may lead to severe side effects, such as retinal hemorrhage and detachment [69].

Previous studies have demonstrated multiple similarities between the BBB and the iBRB. Despite their different site-specific functions, their transport and permeation characteristics have shown to be similar [70,71]. As mammalian retina is readily available from nearby abattoirs, the BRB is more readily used to study different substances crossing the endothelial barrier. Said experimentations can then be used to hypothesize the ability of these substances to cross the BBB.

2.2.2 Mechanism of BBB transport

Substances cross the BBB by one of the following four transport mechanisms: passive diffusion, carrier-mediated transport, adsorptive-mediated transcytosis, and receptor-mediated transport.

2.2.2.1 Passive diffusion

Passive diffusion is a transport mechanism that is only used by small lipid-soluble molecules. These molecules are able to freely diffuse across the BBB by lipid-mediated diffusion. There are not many known substances that use this transport mechanism due to the size limitation and the requirement to be lipophilic, which is an uncommon characteristic [65].

2.2.2.2 Carrier-mediated transport

Carrier-mediated transport (CMT) is one of the most common transport mechanisms used to cross BBB. Substances enter the endothelial cells via their corresponding transmembrane protein on the cell membrane. An example of CMT is the transportation of glucose using glucose transporter type 1 (GLUT1). GLUT1 is able to recognize glucose, as well as mannose and galactose, and actively transport these substances through the BBB [72]. An example of drug delivery using CMT is the delivery of L-DOPA, a drug for Parkinson's Disease, via large neutral amino acid transporter type 1 (LAT1) [73]. LAT1 typically transports phenylalanine, as well as ten other large neutral amino acids, through the BBB.

2.2.2.3 Adsorptive-mediated transcytosis

Adsorptive-mediated transcytosis (AMT) takes advantage of the electrostatic interaction between positively charged ligands and the negatively charged cell membrane. It is mediated by clathrin-dependent endocytosis and is unidirectional from the blood to the brain [65].

2.2.2.4 Receptor-mediated transport

Receptor-mediated transport (RMT) is the other most common transport mechanism. Instead of using a corresponding transmembrane protein as the transporter, peptide receptors on the cell membrane mediate the transcytosis of the ligands [65].

2.2.3 Nanoparticles in Crossing Biological Barriers

Certain specific nanoparticles have shown their ability to cross the BBB. By coupling their BBB crossing abilities and their fluorescent properties, nanomaterials can be modified with specific motifs to act as contrasting agents when performing diagnostic imaging. Various studies have been done to verify their abilities in crossing the BBB and their effectiveness in their role in fluorescent imaging of the brain.

In 2010, Kato and his colleagues demonstrated that bioconjugated QDs were able to cross the BBB to enter the brain parenchyma [74]. The cytotoxic QDs were first conjugated with captopril to improve their biocompatibility and then intraperitoneally administered to rats. After six hours, the QDs were found in various organs and tissues including the brain, although the biodistribution within the brain differed significantly across different rats. The study hypothesized that the smaller QDs were able to cross the BBB while the bigger QDs were unable. Although the exact transport mechanism is unknown, the study suggests the possibility of CMT or the small-sized QDs fitting through the gaps between astrocytic processes and the capillary endothelium. It is also important to note that the bioconjugated QD did not display signs of cytotoxicity during the six hour period in which the rats were kept alive [74].

In 2014, Liu and his colleagues investigated the size dependency of silica nanoparticles when crossing the BBB [75]. The study was first proposed from an older study where

small gold nanoparticles (Au-NPs) were accidentally found to be able to cross the BBB while the larger Au-NPs could not [76]. The study by Liu used an *in vitro* BBB model with a 12-hour incubation period and reported that while all nanoparticles were able to cross the BBB, smaller nanoparticles crossed at a higher concentration compared to larger ones. The study was expanded into an *in vivo* rat model where similar results were shown, with smaller nanoparticles taking less time to cross compared to their larger counterparts [75].

In 2017, Huang and his colleagues demonstrated targeted imaging of glioma and tumor-associated vasculature within the BBB using NGR-conjugated PEG-QD (NGR-QD) [77]. The NGR peptide is known to target CD13 transmembrane glycoprotein, which is overexpressed in tumor cells, and PEG was added to the QD to improve its biocompatibility. Although the study could not determine if NGR-QD was able to cross the BBB, it did successfully bind to glioma and tumor-associated vasculature and was detectable using fluorescence imaging. However, like the previous study by Kato et al., the study maintains that the cytotoxicity of QD cannot be ignored, and only low doses should be administered to ensure low to no toxicity of QDs to animal samples [74,77].

2.2.4 Nanoparticles in Drug Delivery to Biology Barriers

There have been studies of successful drug delivery system using nanoparticles as a vector.

2.2.4.1 AMT transport

The first set of vectors target the AMT transport system for delivery. In a physiological environment, the cerebral endothelial cells are negatively charged due to the polarized distribution of carboxyl groups on glycoprotein and sulfate groups on proteoglycans on the plasma membrane [78,79]. With this in mind, cationic nanoparticles, such as chitosan and certain polymers, have been used to load drugs inside or coat the drugs from the outside [80–83]. Examples of cationic polymers used to load drugs inside are poly(propylene imine) (PPI) and poly(ethylenimine) (PEI) [82,83]. The endocytosis of the drug carrier is completed through AMT. Moreover, the efficiency of AMT can be

amplified by modifying the polymer core with cationic nanoparticles, such as maltodextrin nanoparticles [84].

Apart from taking advantage of the electrostatic interaction, it is also important to note the lipophilic property of the plasma membrane. Naturally, substances with high lipophilicity have easier time interacting with the plasma membrane. A study using solid lipid nanoparticles as a delivery vesicle has also been successful [85].

Unsurprisingly, there are limitations to this delivery method. Cationic surfaces exhibit higher cytotoxic effects compared to their neutral counterparts; furthermore, the AMT transport system is non-specific, which may result in random distribution of the drug instead of targeted treatment [86].

2.2.4.2 RMT transport

Unlike AMT, the binding interaction in RMT is more specific and has higher binding affinity between the ligand and the receptors. As well, the ligand does not need to be positively charged, thereby eliminating the increased potential of cytotoxicity.

Out of the various receptors involved in RMT, transferrin receptors are most often used as they are expressed widely in the luminal membrane of the capillary endothelium [87]. Once the drug is loaded onto the nanoparticle vector of choice, the vector is coated with transferrin so that it can be picked up by the transferrin receptor [88–90].

One major limitation of RMT transport is that there is still a potential for the vector to be delivered to the wrong organ as many receptors are not exclusive to the BBB. The best method for delivery therefore involves taking advantage of both AMT and RMT, by making a nanoparticle vector positively charged as well as coating it with a ligand for receptor-mediated transport. Previous studies have shown that the ligand for RMT can act as a shield to the cationic surface to improve the biocompatibility of the vector while maintaining the electrostatic effects, resulting in successful synergy between RMT and AMT [83].

Chapter 3

3 Self-illumination of Carbon Dots by Bioluminescence Resonance Energy Transfer

3.1 Introduction

Major limitations of *in vivo* fluorescence studies stem from the use of high-power external light source. As mentioned before, the cytotoxicity and tissue damage from the light source results in irreparable damages to the sample; furthermore, tissue autofluorescence and photobleaching lead to inaccurate results.

In order to utilize BRET, which would eliminate problems arising from the external light source, the donor-acceptor pair must be kept in close proximity to one another. While this can be done through protein-protein conjugation between the bioluminescent protein and the fluorescent molecule, CDs are a better candidate compared to other fluorescent molecules as they already have surface functional groups ready for protein conjugation. Moreover, CDs do not denature to lose their fluorescent properties, whereas there is always a potential for proteins to undergo denaturation with the introduction of another molecule through conjugation.

Recently, one study has developed a self-illuminating QD through conjugation of a QD with a synthetic luciferase [11]. While such a recombinant molecule eliminates the need for an external light source, the high toxicity of this QD must be acknowledged for *in vivo* studies. As discussed before, compared to QDs, CDs would be a far superior candidate as a photon acceptor as they exhibit good photostability and high fluorescence intensities like QDs, while also having good biocompatibility, which QDs lack.

Here, we develop a method to produce self-illuminating CDs, which uses the BRET mechanism to achieve its self-illumination. Figure 3 demonstrates the bioconjugation of the CD to Rluc through carboxyl-to-amine crosslinking. The study examines different factors that determine the efficiency of self-illuminating CD production which include: different CD-to-Rluc ratios; two different crosslinkers, N'-(3-dimethylamnopropyl)-N-

ethylcarbodiimide (EDC) and EDC with N-hydroxysuccinimide (NHS); and different conjugation times.

We hypothesize that the BRET efficiency would be superior when conjugating Rluc and CD using EDC/NHS compared to only EDC, as EDC/NHS is a more potent coupler compared to EDC. Furthermore, we also hypothesize that BRET efficiency would increase with higher concentrations of the CD and longer conjugation times, as more conjugation would allow for more self-illuminating CDs to be produced, therefore increasing the BRET efficiency of the sample.

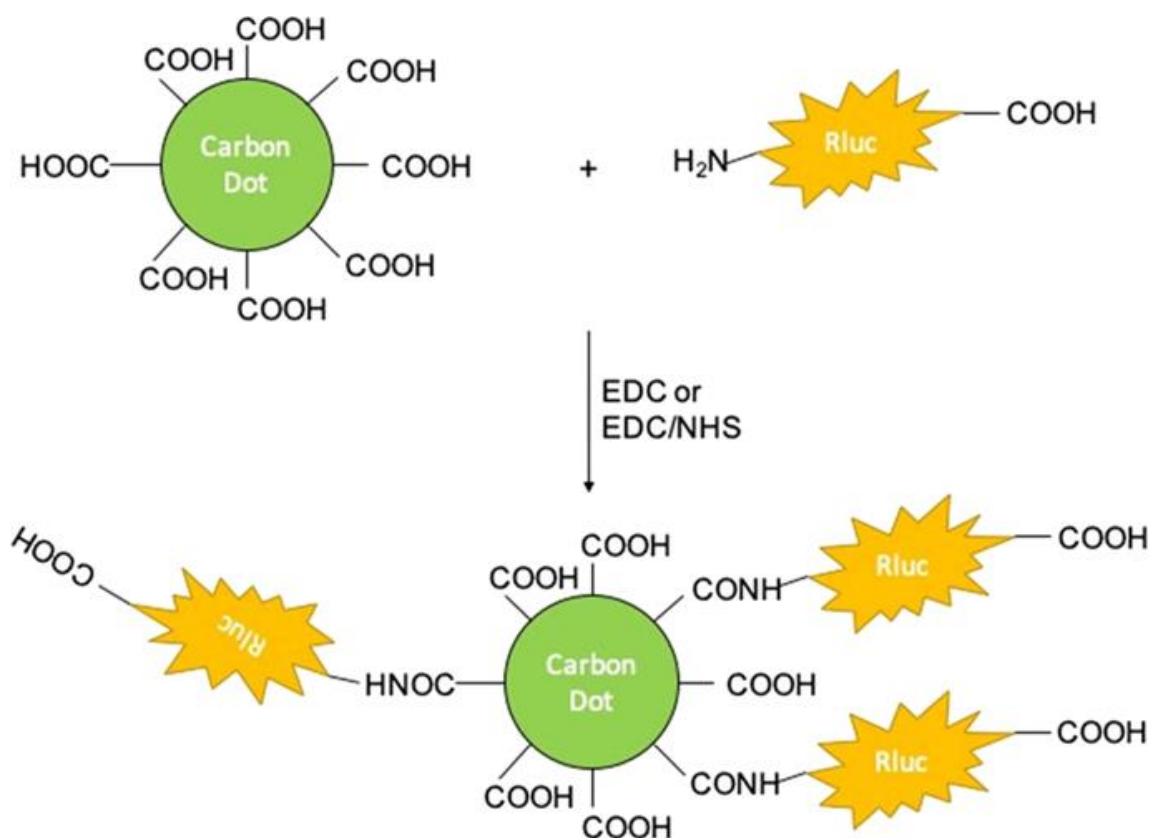


Figure 3: EDC- or EDC/NHS-mediated conjugation of bioluminescent protein, Rluc to CDs. Both crosslinkers couple the free surface carboxylic acids on the CD with the amine group on the N-terminal of Rluc to form peptide bond. The close proximity between CD and Rluc after conjugation allows for BRET.

3.2 Materials and Methods

3.2.1 Materials

Citric acid, urea, EDC, and NHS were purchased from Sigma Aldrich (Oakville, Canada). Rluc and CTZ were purchased from Nanolight Technology (Pinetop, USA).

3.2.2 Carbon Dot Synthesis

This method was derived from a previously reported method, which utilizes a microwave oven-assisted process to produce water-soluble CDs [11]. Citric acid and urea were added to excess distilled water in 1:1 ratio. The solution was heated using a domestic 750 W microwave oven in 45 second intervals until it became dark brown clustered solid. The resulting solid was cooled to room temperature then frozen overnight. The frozen solid was then freeze dried (The Virtis Company, Gardiner, USA) for two days in order to isolate the CDs.

3.2.3 Bioconjugation of *Renilla* Luciferase with Carbon Dot

Two different sets of samples were prepared: one set using 10 μ L of 20 mM EDC and the other using 10 μ L of 20 mM EDC and 10 μ L of 20 mM NHS. Each set consisted of five different samples of different concentrations of CDs dissolved in distilled water: 0.10 mg/mL, 0.20 mg/mL, 0.40 mg/mL, 0.80 mg/mL, and 1.20 mg/mL. The final volume of each samples was 400 μ L, and all samples were incubated for 30 min at 37 °C. 2 μ M Rluc was added to each sample then further incubated at 37 °C for 1 hour. Samples were used immediately for fluorescence study after the incubation. The procedure was repeated twice with different incubation periods: 6.5 hours and 24 hours.

3.2.4 Photoluminescence Study

All fluorescence measurements were obtained using PTI Fluorescence Master System (HORIBA Canada Inc.). Emission spectra from 400 nm to 700 nm of the CD and Rluc were measured. The excitation wavelength was set to 480 nm, the emission wavelength of Rluc, when measuring the emission spectrum of CD. 30 μ M CTZ was added to Rluc immediately before measuring the emission spectrum of Rluc to initiate bioluminescence.

Due to the short-lived nature of Rluc bioluminescence, the step size was fixed at 10 nm, and the integration was fixed at 0.1 s for all measurements. Bioluminescence of Rluc as a function of time after CTZ introduction can be found in Appendix 3.

Immediately prior to taking the measurements, 30 μM CTZ was added to the samples to initiate the BRET mechanism. Emission spectrum for each sample was then measured from 400 nm to 700 nm with the external light source turned off.

3.3 Results

3.3.1 Bioluminescence of *Renilla* Luciferase and Photoluminescence of Carbon Dot

The maximum bioluminescence intensity of Rluc (2.0 μM) was observed at 480 nm as shown in Figure 4a. The small inset in Figure 4a demonstrates the 37.5 kDa Rluc on SDS-PAGE gel. The bioluminescence of Rluc increased linearly as the concentration of CTZ increased from 0 μM to 13.6 μM and then plateaued with higher concentration of CTZ following the Michaelis-Menten model as shown in Figure 4b. Michaelis constant (K_m) was calculated to be 2.83 μM ; therefore, 30 μM CTZ was used for 2 μM Rluc as it is normal to add substrate within 10–20 times of K_m to reach maximum reaction velocity.

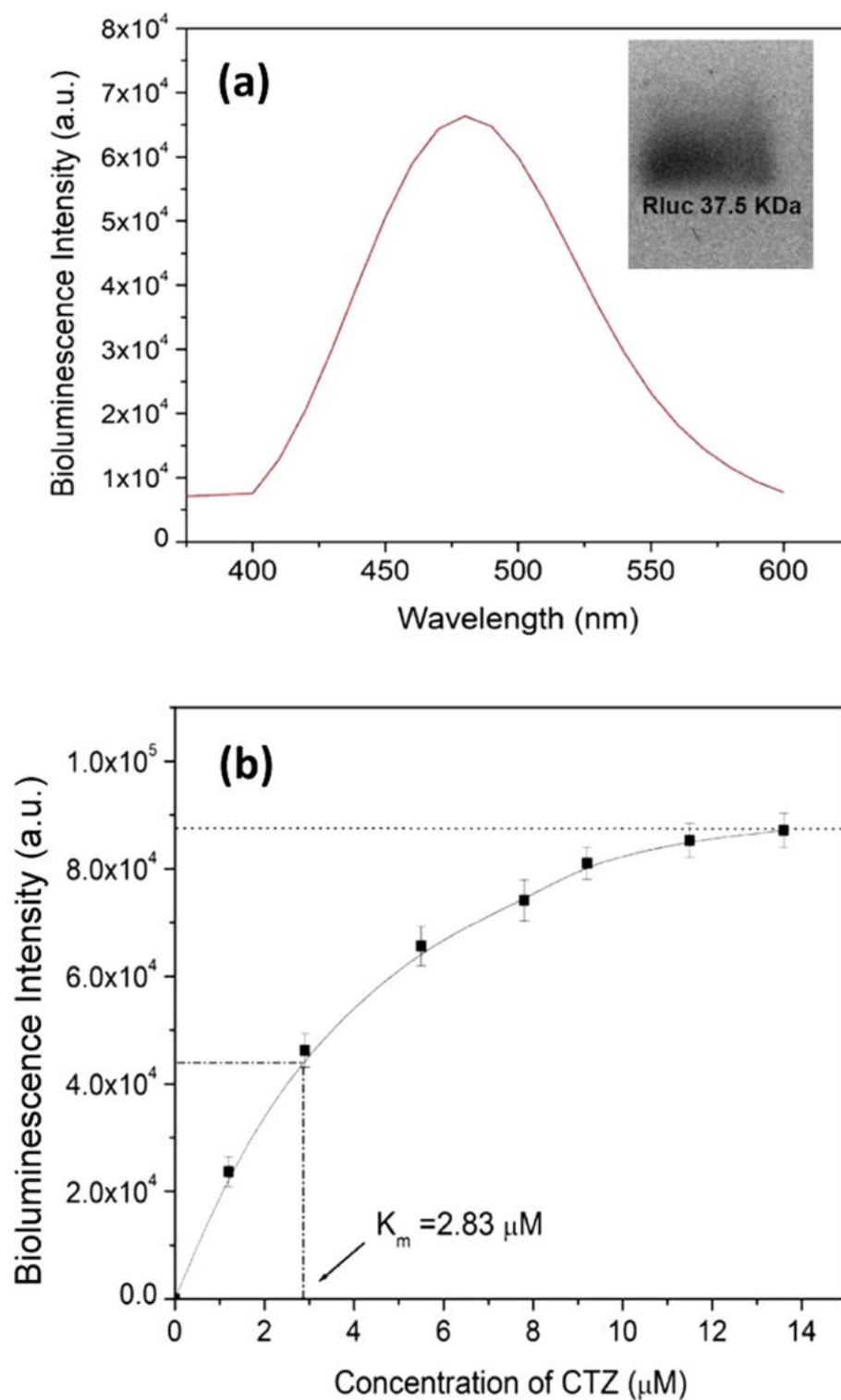


Figure 4: (a) Bioluminescence of $2.0 \mu\text{M}$ Rluc reacting with $7.8 \mu\text{M}$ CTZ. The small inset shows the purified Rluc on the SDS-PAGE gel. (b) Bioluminescence intensity as a function of the concentration of CTZ, its substrate.

Due to the small nature of the CD, CD characterization was done using TEM as shown in the small inset of Figure 5, with average particle size being estimated at 13 ± 3 nm. The photoluminescence of free CD is shown in Figure 5, and the UV-vis absorption spectra of CDs at different concentrations is shown in Appendix 1. All CD samples displayed broad absorption spectra with the same absorbance peaks at 270 nm, 340 nm, and 405 nm, which matches the absorbance peaks reported in previous study; furthermore, the CDs have excitation-wavelength-dependent PL properties within maximum yield at about 14% [20]. Since the emission of Rluc is centered at 480 nm, the photoluminescence of CD was measured with an excitation wavelength of 480 nm. The maximum emission of CD was observed to be around 557 nm as shown in Figure 5.

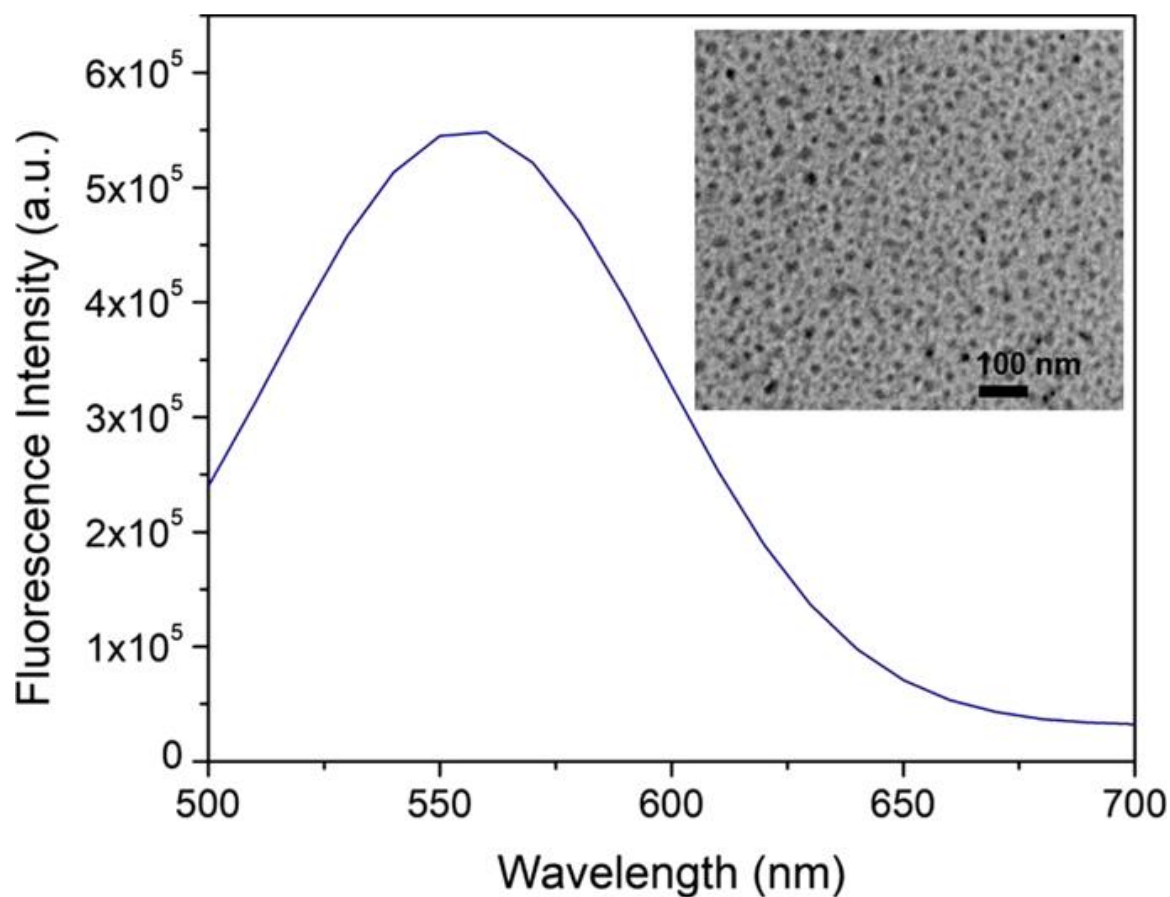


Figure 5: Photoluminescence of CDs under an excitation wavelength of 480 nm. TEM micrograph of CDs is shown in the small inset of the figure.

3.3.2 The Factors on the Performance of BRET

3.3.2.1 EDC- and EDC/NHS-mediated conjugations

Two crosslinking agents, EDC and EDC/NHS, were used to conjugate Rluc onto CDs through amide bond. Conjugation time frame was fixed at 6.5 hours while the concentration of the CD was also fixed at 0.20 mg/mL. The resulting emission spectra can be seen in Figure 6. While the samples conjugated with EDC retained a broad peak, a complete loss of fluorescence can be observed for samples conjugated with EDC/NHS.

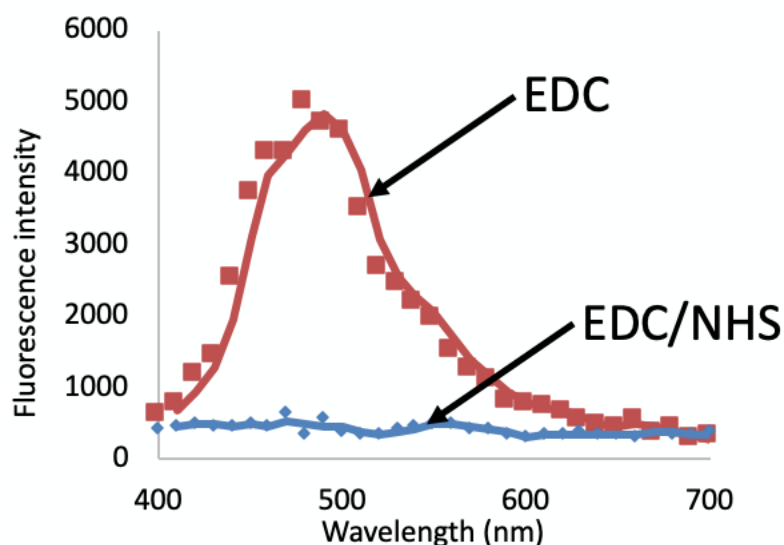


Figure 6: Emission spectra of EDC- and EDC/NHS-mediated conjugation of Rluc and CD. The concentration of CD was fixed at 0.20 mg/mL, and the conjugation time was fixed at 6.5 hours.

3.3.2.2 Different concentrations of CD

Five different concentrations of CD were used to produce self-illuminating CD: 0.10 mg/mL, 0.20 mg/mL, 0.40 mg/mL, 0.80 mg/mL and 1.20 mg/mL. Emission spectrum from three of the five concentrations of CD are shown in Figure 7. The conjugation time was fixed at 6.5 hours and EDC was used as the conjugation factor. A sharp peak can be observed from the sample using 0.10 mg/mL, while a broad peak can be observed from the sample using 0.20 mg/mL. Although not pictured, 0.40 mg/mL and 0.80 mg/mL

displayed broad peak similar to that shown in 0.20 mg/mL. Lastly, the sample using 1.20 mg/mL had complete loss of fluorescence.

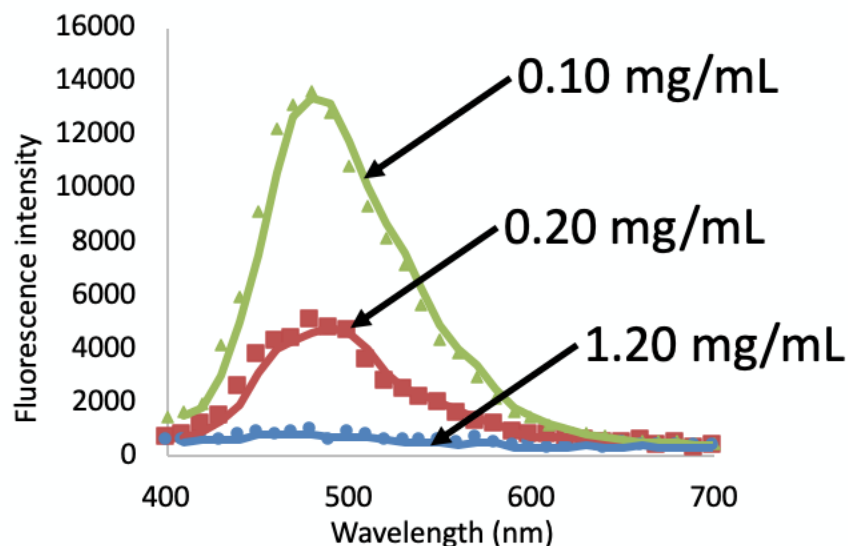


Figure 7: Emission spectra of samples using different concentrations of CDs. EDC was used as the coupling agent, and the conjugation time was fixed at 6.5 hours.

3.3.2.3 Different conjugation times

Three different conjugation times were used when conjugating Rluc to the CD: 1 hour, 6.5 hours, and 24 hours. The concentration of the CD was fixed at 0.20 mg/mL, and EDC was used as the coupling agent for the conjugation. The resulting emission spectrum is shown in Figure 8. One sharp peak is observed for 1 hour conjugation; a broad peak is observed for 6.5 hours of conjugation; and finally, a lack of peak is observed for 24 hours.

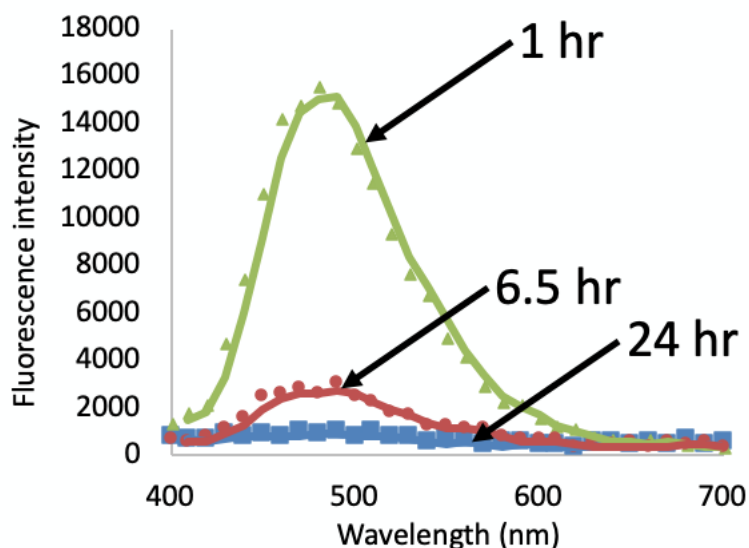


Figure 8: Emission spectra of samples produced using different conjugation times. The concentration of the CD was fixed at 0.20 mg/mL, and EDC was used as the coupling agent.

3.3.2.4 BRET profile and efficiency of BRET

Figure 9a displays the BRET profile of 6.5 hours of conjugation of 2.0 μ M Rluc and 0.20 mg/mL CD with EDC as coupling agent. The black line is the emission measurement taken using the sample, while the red and blue lines, which represent Rluc and CD respectively, were obtained by using multi-peak fitting software. The small inset of Figure 9a is photos of Rluc compared to CD-Rluc, the self-illuminating CD without any external high-power light supply. BRET profiles of 6.5 hours of conjugation of 2.0 μ M Rluc and 0.40 mg/mL CD and 0.08 mg/mL CD with EDC as the coupling agent can be found in Appendix 2.

BRET efficiency was calculated using the following equation [11]

$$E_{BRET} = \frac{I_{CDs}}{I_{Rluc}},$$

where I_{CDs} is the integrated emission within the range of 450–650 nm from CDs caused by the BRET, and I_{Rluc} is the integrated emission within the range of 390–550 nm from

bioluminescence of Rluc. Higher BRET efficiency represents better energy transfer from Rluc to CDs. Figure 9b shows that the BRET efficiency increases linearly with increasing concentrations of CDs from 0.20 mg/mL to 0.80 mg/mL.

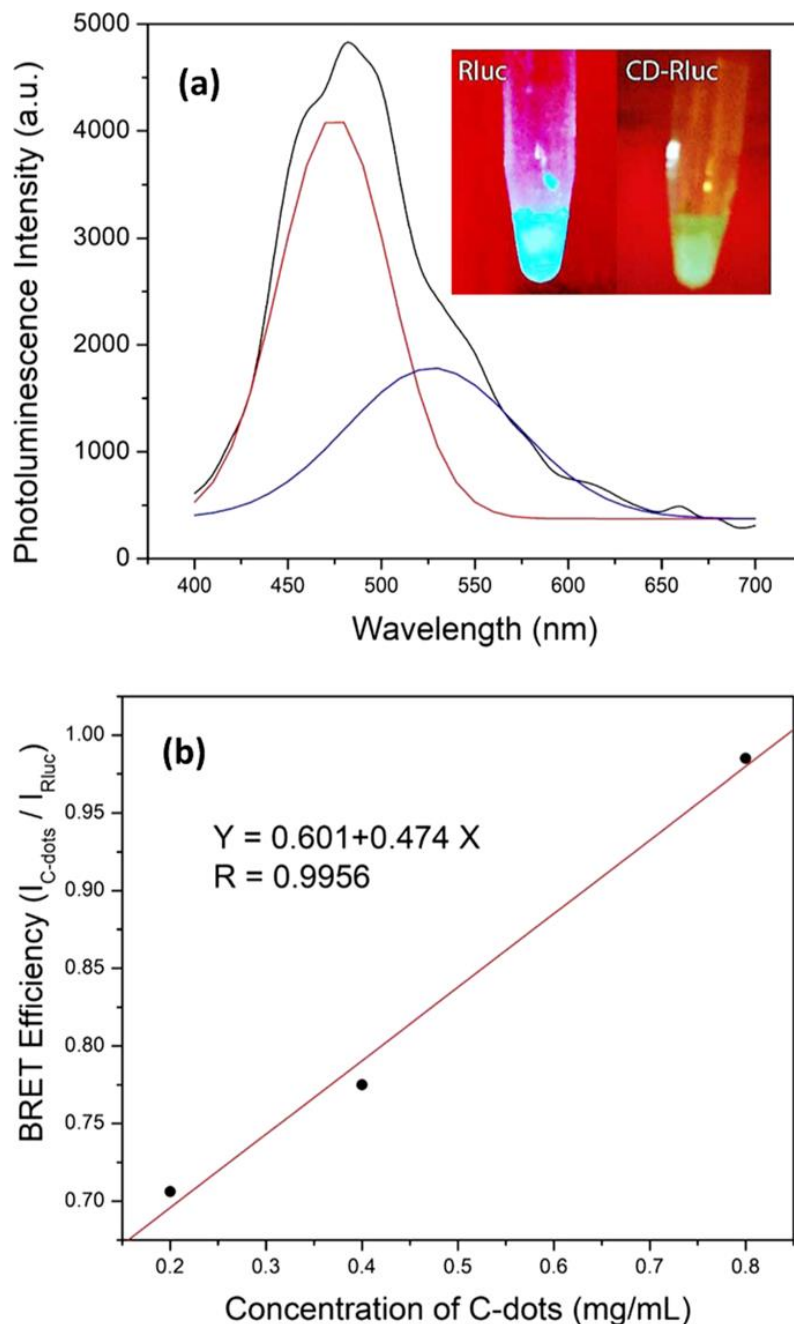


Figure 9: (a) BRET profile of sample made using EDC as coupling agent with 0.20 mg/mL of CD and 2 μ M Rluc for 6.5 hours of incubation. The black line represents the emission spectrum of the sample, or the BRET profile. The red and blue line,

which represents Rluc and CD respectively, were obtained using multi-peak fitting software. The small inset is the photo of 2 μ M Rluc and CD-Rluc complex. (b) BRET efficiency as a function of CD concentration.

3.4 Discussion

It is no with doubt that the bioconjugation of Rluc to CD is vital to achieve the self-illuminating CD through the BRET mechanism. Surprisingly, we observed that EDC/NHS conjugation resulted in a complete loss of fluorescence. It is important to note that both EDC- and EDC/NHS-mediated conjugation is non-selective in that the coupling agents conjugate any free carboxylic acid to any free amine group. Because of their non-selective nature, conjugation can occur between the carboxylic acid group on the CD with either the amine on the N-terminal of Rluc or the amine on lysine residues of the Rluc [91]. Because Rluc is a small protein, conjugation of the CD in the middle of the protein may lead to denaturation as described in previous literature using different small proteins [54,92]. Furthermore, a previous study demonstrated that protein conjugation at lysine residues of Rluc may be fatal to protein structure and may result in loss of function [91]. Another study has already shown that mutations involving certain lysine residues of Rluc led to decreased in function to further support this event [93].

A similar problem may have arisen with high CD concentration and longer conjugation period. We observed that fluorescence is completely lost with CD concentration of 1.20 mg/mL and conjugation time of 24 hours. With more CD present, there would have been a higher possibility of more CD-lysine residue conjugation, leading to loss of fluorescence. Similarly, with longer conjugation time, there would be an increased potential for CD to conjugate at lysine residues as well as the N-terminal of Rluc. Although EDC is a less potent coupling agent, with high enough concentration of the CD and long enough conjugation time, conjugation at lysine residues of Rluc are not preventable as supported by experimental data.

On the other hand, no BRET phenomenon is observed for low concentration of the CD and short conjugation time. Only a sharp peak representing the Rluc fluorescence can be observed as seen in Figures 5 and 6. This can be explained by the kinetic nature of bond

formation. For bonds to form, molecules must collide with one another at a correct angle; however, with low concentration of the CD, the probability of collision decreases, and with short conjugation time, the potential for collision also decreases.

The BRET phenomenon was observable for 0.20–0.80 mg/mL of CD conjugated with 2 μ M Rluc with EDC as coupling agent for 6.5 hours of conjugation. The BRET efficiency was observed to be linearly correlated within the said range of CD concentrations. As mentioned earlier, when the concentration of the CD is increased beyond 0.80 mg/mL, the fluorescence function of Rluc is lost due to overwhelming conjugation at the lysine residue. Previous studies of BRET using organic dyes conjugated with a bioluminescence protein also showed that non-specific BRET signals tend to increase linearly with increasing acceptor concentrations [94,95].

3.5 Conclusion

In conclusion, water-soluble CDs with average particle size of 13 ± 3 nm were produced using microwave oven-assisted process. In order to achieve self-illumination of the CD, Rluc, a bioluminescent protein, was conjugated onto the CDs, as the BRET mechanism is distance dependent. Rluc bioluminesces at 480 nm, which falls within the range of the CD absorption spectrum. CD emits at 557 nm when excited with a photon at 480 nm. The ideal concentration of Rluc substrate, CTZ, was investigated, and the Michaelis constant was calculated to be around 2.83 μ M when using 2 μ M Rluc. Three different factors leading to conjugation were investigated: different coupling agents, different concentrations of the CD, and different conjugation times. Our study indicated that BRET efficiency increases linearly with increasing concentrations of CD from 0.20 mg/mL to 0.80 mg/mL with EDC as the conjugating agent at 6.5 hours of conjugation.

Chapter 4

4 Investigation of Carbon Dot Crossing Bovine Blood Retina Barrier

4.1 Introduction

With an increasing population suffering from various neurodegenerative diseases and retinal degenerative diseases, it is crucial to investigate different methods of diagnosing and treating such diseases. The first step in the development of these methods would be to uncover more substances that are able to successfully cross the biological barriers.

Although different nanoparticles have been shown to cross the BBB, there are limitations observed in such studies. QDs are known to be cytotoxic and therefore are not ideal for *in vivo* studies. Although such a problem can be resolved by coating the QD with biocompatible materials, there is potential for the biocompatible material to degrade faster than the QD, which would lead to exposure of the toxic material. Though silica nanoparticles are biocompatible, they are not fluorescent and require an additional step to load them with traditional dyes.

CDs would be an ideal candidate for the study as they are fluorescent and biocompatible; furthermore, it is easy to modify CDs through surface conjugation for targeted studies. The present study aims to investigate if CDs are able to cross biological barriers. As bovine retina is easier to obtain compared to an intact bovine BBB system, bovine retina will be used to represent the biological barrier system for this investigation.

4.2 Materials and Methods

4.2.1 Materials

Citric acid, urea, sterile phosphate buffered saline (PBS), and Triton X-100 were purchased from Sigma Aldrich (Oakville, Canada). Bovine eyes were graciously donated by Mount Brydges Abattoir (London, Canada).

4.2.2 Carbon Dot Synthesis

This method was derived from a previously reported method, which utilizes a microwave oven-assisted process to produce water-soluble CDs [11]. Citric acid and urea were added to excess distilled water in 1:1 ratio. The solution was heated using domestic 750 W microwave oven in 45 second intervals. The solution was heated until it became dark brown clustered solid. The resulting solid was cooled to room temperature then frozen overnight. The frozen solid was then freeze dried (The Virtis Company, Gardiner, USA) for two days in order to isolate the CDs.

4.2.3 Preparation of Bovine Retina

The following protocol was derived from previous studies [96,97]. Fresh bovine eyes were obtained from the local abattoir and used within 3 hours. First, extraocular tissue was removed from the eyes. The images of bovine eyes before and after extraocular tissue removal is shown in Figure 10. An incision of 8–10 mm was made along the border of the cornea and sclera using a surgical blade. The incision was extended around the entire eye using scissors, and the anterior segment and the vitreous was separated from the neural retina. The resulting structure will be referred to as “eye cup” from herein forward. An image of eye cup is shown in Figure 11. 1 mL of 1mg/mL CD in distilled water was added to the inside of the eye cup. The eye cup was incubated for 1.5 hours at 37 °C. After the incubation, the CD solution was removed from the eye cup, and the inside was rinsed three times using 3 mL of distilled PBS. From the inside, the neural retinal layer was peeled from the eye cup and placed in the tissue grinder tube on ice. Next, the choroid layer was peeled from the eye cup and placed in another tissue grinder tube on ice. Both tissue samples were then homogenized on ice in 500 μ L PBS containing 2% Triton X-100. The samples were centrifuged at 5000 rpm for 20 minutes at 4 °C, and the supernatants were collected and placed on ice in preparation for fluorescence study.

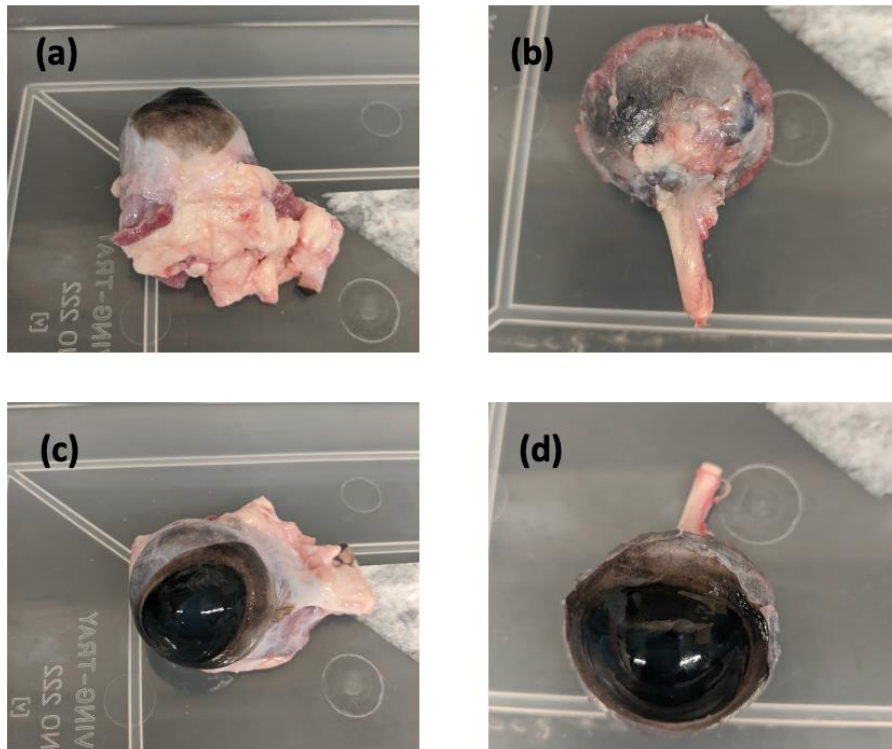


Figure 10: (a) Back of the bovine eye before extraocular tissue removal. (b) Back of the bovine eye after extraocular tissue removal. (c) Front of the bovine eye before extraocular tissue removal. (d) Front of the bovine eye after extraocular tissue removal.

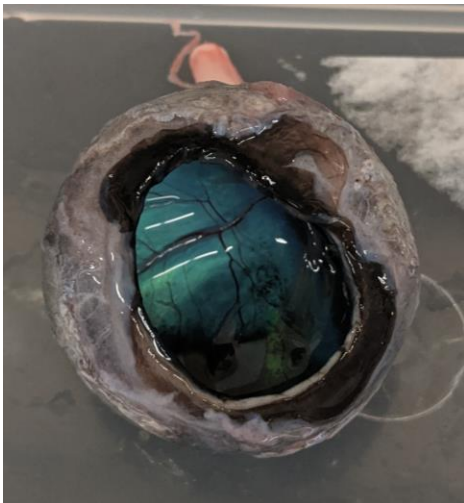


Figure 11: Experimental eye cup. Extraocular tissues have been removed and, the anterior segment and the vitreous are removed in preparation for CD treatment.

4.2.4 Fluorescence Study

All fluorescence measurements were obtained using PTI Fluorescence Master System (HORIBA Canada Inc.), and the excitation wavelength was fixed at 430 nm, where it corresponds with the highest absorption peak of CD (See Appendix 1). First, the emission spectrum of the CD was measured. The emission spectra of the neural retinal layer and the choroid layer without any treatment were measured. The emission spectra of all samples were then measured.

4.3 Results

4.3.1 Neural Retinal Layer

Figure 12 shows three lines: the green dotted line representing free CD, the blue line representing the neural retina layer before CD treatment, and the orange line representing the neural retina layer after CD treatment. In the initial CD photoluminescence spectrum, one peak was observed centered at 530 nm. No distinct peak was observable in the neural retina layer prior to CD treatment, although some fluorescence was observed. The neural retina layer after CD treatment displayed a distinct peak also centered at 530 nm as seen in the free CD spectrum.

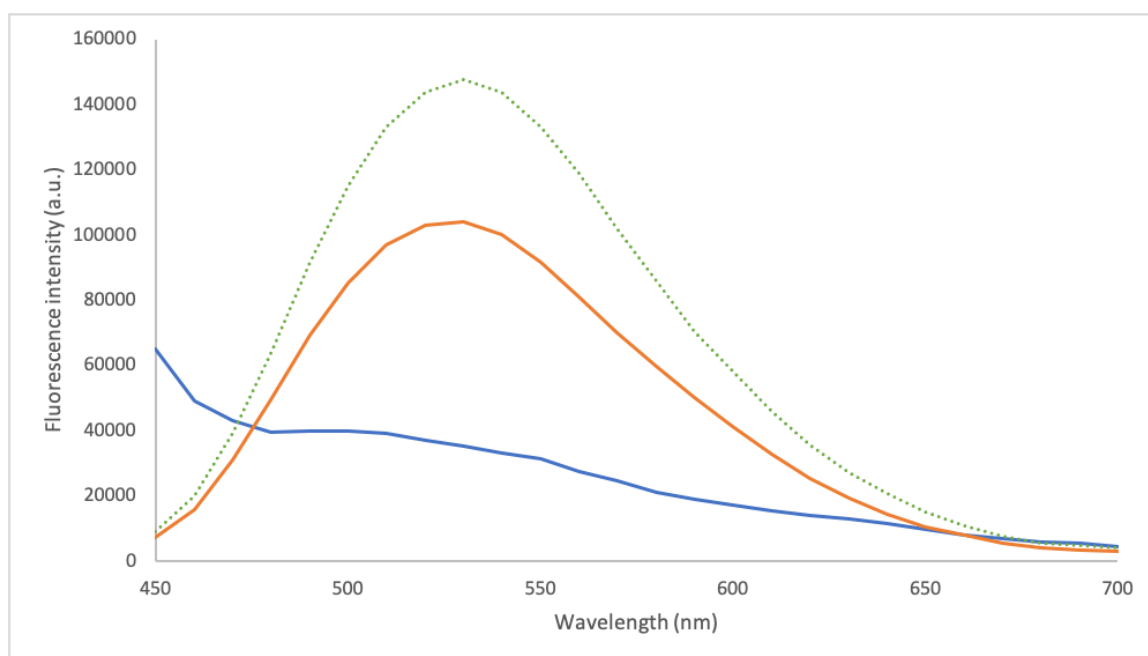


Figure 12: Emission spectra of free CD (green), neural retinal layer before CD treatment (blue), and neural retinal layer after CD treatment (orange). CD treatment consisted of 1 mL of 1 mg/mL CD incubated for 1.5 hours inside the eye cup.

4.3.2 Choroid Layer

Figure 13 shows three lines: the green dotted line representing free CD, the blue line representing the choroid layer before CD treatment, and the orange line representing the choroid layer after CD treatment. In the initial CD photoluminescence spectrum, one peak was observed centered at 530 nm. Although no sharp peaks were observable in the choroid layer prior to CD treatment, two weak and broad peaks can be observed centered around 500 nm and 590 nm. The choroid layer after CD treatment displayed a broad fluorescent area with three peaks centered around 500 nm, 530 nm, and 590 nm.

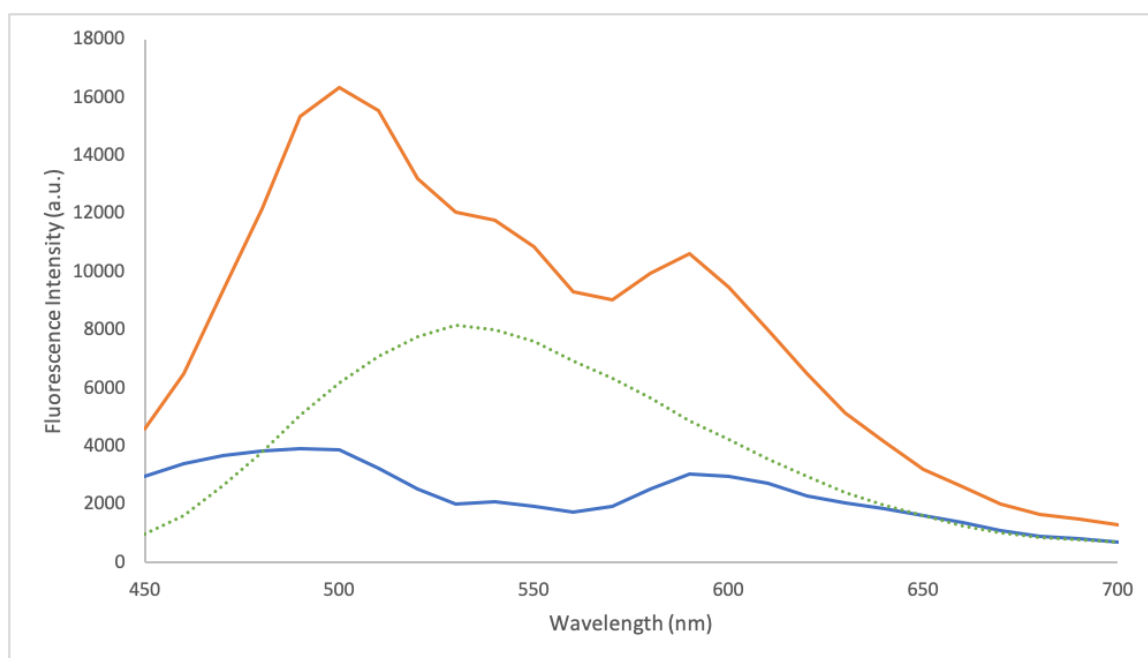


Figure 13: Emission spectra of free CD (green), choroid layer before CD treatment, (blue) and choroid layer after CD treatment (orange). CD treatment consisted of 1 mL of 1 mg/mL CD incubated for 1.5 hours inside the eye cup.

4.4 Discussion

By only observing the results from the neural retina layer, it is not possible to conclude if the CD was successful in crossing the BRB. Because the CD was incubated inside the eye cup, there is potential for the CD to stick to the endothelial cells of the neural retina layer. As seen in Figure 12, the emission spectrum of the neural retina layer after CD treatment displays fluorescent peak that corresponds to the CD emission spectrum, although there is a decrease in fluorescence intensity. The decrease in fluorescence intensity could have resulted from the CD that did not cross or adhere to the neural retina layer. It is worthwhile to note that when comparing the emission spectra of the neural retina layer before and after the CD treatment, there is a loss of fluorescence at certain wavelengths after the treatment. While certain pigments may have been lost during the tissue homogenization process, studies investigating the relationship between CDs and the maintenance of BRB structure should be performed.

The results from the choroid layer are surprising, as it seems that some CD was able to cross over the neural retina layer into the choroid layer. It is also interesting that while the some of the initial fluorescence of neural retina layer was lost after CD treatment, the initial fluorescence of choroid layer seems to be amplified by the CD fluorescence signal. When observing the emission spectrum of the choroid layer after the CD treatment, three peaks can be observed; two peaks, which match the initial weaker peaks seen in the choroid layer, and the middle peak, which corresponds with the CD emission peak.

4.5 Conclusion

In summary, the study investigated the ability of CDs to cross biological barriers. Due to the readily available nature of bovine eyes, the BRB model was used to perform this study. While it was not surprising to receive CD emission signals from the neural retina layer after CD treatment of the inside of the eye, it is interesting to be able to observe CD fluorescence signal from the choroid layer, which signifies that CD had to cross over the neural retina layer in order to be present in the choroid layer. The neural retina layer represents the iBRB, which has been shown to be similar to the BBB in structure and permeability; therefore, it would be of interest to conduct similar studies with a BBB

model to examine if the CD is able to also cross the BBB. More supporting data would be required to conclude that CDs can indeed cross biological barriers; however, this investigation acts as a steppingstone for further examination.

Chapter 5

5 Summary and Future Work

5.1 Summary

FNPs are good candidates for fluorescence studies due to their brightness, good photostability, good biodistribution, and easily modifiable surface. In particular, CDs are ideal amongst the FNPs due to their biocompatibility and the different excitation-emission pairings available. Although CDs can be used freely in the majority of fluorescence studies, two studies were performed in order to open new doors for CDs to be used in further fluorescence studies.

The first investigation consisted of the development of self-illuminating CDs. For many fluorescence studies, especially the ones that examine protein-protein interactions, FRET is the most commonly used method. Although FRET is distance dependent and therefore useful when studying the interactions between two molecules, the necessity of a high-power external light source poses many limitations, such as photocytotoxicity, tissue damage, photobleaching, and autofluorescence. Such limitations can result in inaccurate data as well as cause irreparable damage to the sample. A self-illuminating CD, which uses the BRET mechanism instead of FRET, eliminates the need for a high-power external light source, thereby resolving all limitations stemming from it. The development of a self-illuminating CD involved three different factors: different coupling agents, different CD concentrations, and different conjugation times. The ideal conditions for developing a self-illuminating CD was found to be 6.5 hours of conjugation using EDC as the coupling agent with 0.20–0.80 mg/mL of CD. The BRET efficiency was calculated and observed to be linearly correlated with increasing concentrations of CD.

The second investigation was an examination of the ability of CDs in crossing biological barriers. Two different barriers were introduced: the BBB and the BRB. Each barrier, while extremely crucial in normal settings, also poses difficulties when diagnosing and treating degenerative diseases of the brain or the retina. The rare ability to cross these biological barriers is significant as it opens potential for the development of diagnostic

tools as well as a drug delivery system to structures beyond the barriers. Although different NPs have been found to be able to cross the BBB, CDs have yet to be studied. CDs would be an ideal candidate for studying the biological barrier due to their fluorescence characteristics and good biocompatibility. Because of the readily available nature of bovine eyes from abattoirs, the BRB model was used to study the ability of CDs in crossing biological barriers. Although the fluorescence studies conducted in this investigation suggests that CDs are able to cross the iBRB into the oBRB, more supporting data using different methods would be necessary before concluding that CDs are able to cross biological barriers.

The introduction of a self-illuminating CD and the potential of CDs in crossing biological barriers opens new doors in the biomedical field of research. The first leads to *in vivo* studies where the external light source is problematic; and the second leads to studies involving biological barriers, whether they involve diagnosis or drug delivery.

5.2 Limitations and Future Work

5.2.1 Self-illuminating CD

The major limitation in the self-illuminating CD study is the lack of methods to isolate the self-illuminating CD from the sample, which consists of free Rluc, free CD, and the self-illuminating CD. After the conjugation step is completed, there would be unconjugated Rluc and CD left over. To use the self-illuminating CD in fluorescence studies, isolation and purification of the CD would be necessary to ensure high concentration and lack of impurities that could interfere with the results.

Furthermore, although Rluc was used as the bioluminescent protein for the BRET pairing, recently synthetically developed luciferases have even better photostability as well as brighter intensities while being smaller in size. As well, the substrate used by these new luciferases is also different and have shown better biodistribution and stability in *in vivo* settings. Future work could involve switching out Rluc for these newer alternatives to make a more powerful self-illuminating CD.

More generally, the compatibility of the CD and bioluminescent proteins opens new doors in developing non-invasive biosensors. As BRET is distance dependent, combination of a multicolor CD and the BRET technique could be used in conjunction to measure protein-protein or protein-nucleic acid interactions.

5.2.2 CD crossing BRB

The major limitation in this study is the lack of supporting evidence to demonstrate that CDs can cross the BRB. Further studies involving TEM or SEM imaging to visualize the CD in the different layers of BRB would be interesting and act as a strong supporting evidence. More studies should be conducted to investigate if the presence of the CD results in damage in the neural retina layer, as loss of fluorescence in the neural retina layer after the CD treatment could be observed in Figure 13.

If the CD is able to cross the biological barrier, it would be interesting to see if the self-illuminating CD could also cross the barrier. As discussed before, fluorescence imaging involving an external light source usually leads to inaccurate results and irreparable damages to the samples. It would be beneficial to be able to use BRET techniques in order to conduct these fluorescent studies compared to traditional FRET techniques or fluorescent imaging.

Targeting studies with CDs would be easier to implement as CDs have multiple surface groups that are ready to be conjugated without potentially losing its fluorescence. Similar to a study by Huang and his colleagues, CDs could be modified with specific ligands for receptors that are overexpressed in cancerous cells [77]. Because CDs exhibit far greater biocompatibility compared to QDs, they would be an ideal substitute for such *in vivo* studies.

5.3 References

1. Mohanraj, V.J.; Chen, Y. Nanoparticles - A review. *Trop. J. Pharm. Res.* **2006**, *5*, 561–573, doi:10.4314/tjpr.v5i1.14634.
2. S. Wolfbeis, O. An overview of nanoparticles commonly used in fluorescent bioimaging. *Chem. Soc. Rev.* **2015**, *44*, 4743–4768, doi:10.1039/C4CS00392F.

3. Ruedas-Rama, M.J.; Walters, J.D.; Orte, A.; Hall, E.A.H. Fluorescent nanoparticles for intracellular sensing: A review. *Anal. Chim. Acta* **2012**, *751*, 1–23, doi:10.1016/j.aca.2012.09.025.
4. Somers, R.C.; Bawendi, M.G.; Nocera, D.G. CdSe nanocrystal based chem-/bio-sensors. *Chem. Soc. Rev.* **2007**, *36*, 579–591, doi:10.1039/B517613C.
5. Lin, C.-A.; Liedl, T.; Sperling, R.; Pereiro, R.; Sanz-Medel, A.; Chang, W.; Parak, W. Bioanalytics and biolabeling with semiconductor nanoparticles (quantum dots). *J. Mater. Chem. - J MATER CHEM* **2007**, *17*, doi:10.1039/b618902d.
6. Dubertret, B.; Skourides, P.; Norris, D.J.; Noireaux, V.; Brivanlou, A.H.; Libchaber, A. In vivo imaging of quantum dots encapsulated in phospholipid micelles. *Science* **2002**, *298*, 1759–1762, doi:10.1126/science.1077194.
7. Frasco, M.F.; Chaniotakis, N. Semiconductor quantum dots in chemical sensors and biosensors. *Sensors* **2009**, *9*, 7266–7286, doi:10.3390/s90907266.
8. Ruedas-Rama, M.J.; Wang, X.; Hall, E.A.H. A multi-ion particle sensor. *Chem. Commun.* **2007**, 1544–1546, doi:10.1039/B618514B.
9. Li, K.; Pan, J.; Feng, S.-S.; Wu, A.W.; Pu, K.-Y.; Liu, Y.; Liu, B. Generic Strategy of Preparing Fluorescent Conjugated-Polymer-Loaded Poly(DL-lactide-co-Glycolide) Nanoparticles for Targeted Cell Imaging. *Adv. Funct. Mater.* **2009**, *19*, 3535–3542, doi:10.1002/adfm.200901098.
10. Yang, H.; Zhuang, Y.; Hu, H.; Du, X.; Zhang, C.; Shi, X.; Wu, H.; Yang, S. Silica-Coated Manganese Oxide Nanoparticles as a Platform for Targeted Magnetic Resonance and Fluorescence Imaging of Cancer Cells. *Adv. Funct. Mater.* **2010**, *20*, 1733–1741, doi:10.1002/adfm.200902445.
11. So, M.-K.; Loening, A.M.; Gambhir, S.S.; Rao, J. Creating self-illuminating quantum dot conjugates. *Nat. Protoc.* **2006**, *1*, 1160–1164, doi:10.1038/nprot.2006.162.
12. Danek, M.; Jensen, K.F.; Murray, C.B.; Bawendi, M.G. Synthesis of Luminescent Thin-Film CdSe/ZnSe Quantum Dot Composites Using CdSe Quantum Dots Passivated with an Overlayer of ZnSe. *Chem. Mater.* **1996**, *8*, 173–180, doi:10.1021/cm9503137.

13. Nordell, K.J.; Boatman, E.M.; Lisensky, G.C. A Safer, Easier, Faster Synthesis for CdSe Quantum Dot Nanocrystals. *J. Chem. Educ.* **2005**, *82*, 1697, doi:10.1021/ed082p1697.
14. Zhou, J.; Zhou, H.; Tang, J.; Deng, S.; Yan, F.; Li, W.; Qu, M. Carbon dots doped with heteroatoms for fluorescent bioimaging: a review. *Microchim. Acta* **2017**, *184*, 343–368, doi:10.1007/s00604-016-2043-9.
15. Li, S.; Luo, J.; Yin, G.; Xu, Z.; Le, Y.; Wu, X.; Wu, N.; Zhang, Q. Selective determination of dimethoate via fluorescence resonance energy transfer between carbon dots and a dye-doped molecularly imprinted polymer. *Sens. Actuators B Chem.* **2015**, *206*, 14–21, doi:10.1016/j.snb.2014.09.038.
16. Zuo, P.; Lu, X.; Sun, Z.; Guo, Y.; He, H. A review on syntheses, properties, characterization and bioanalytical applications of fluorescent carbon dots. *Microchim. Acta* **2016**, *183*, 519–542, doi:10.1007/s00604-015-1705-3.
17. Sun, Y.-P.; Zhou, B.; Lin, Y.; Wang, W.; Fernando, K.A.S.; Pathak, P.; Mezziani, M.J.; Harruff, B.A.; Wang, X.; Wang, H.; et al. Quantum-Sized Carbon Dots for Bright and Colorful Photoluminescence. *J. Am. Chem. Soc.* **2006**, *128*, 7756–7757, doi:10.1021/ja062677d.
18. Hu, S.; Liu, J.; Yang, J.; Wang, Y.; Cao, S. Laser synthesis and size tailor of carbon quantum dots. *J. Nanoparticle Res.* **2011**, *13*, 7247–7252, doi:10.1007/s11051-011-0638-y.
19. Guan, W.; Gu, W.; Ye, L.; Guo, C.; Su, S.; Xu, P.; Xue, M. Microwave-assisted polyol synthesis of carbon nitride dots from folic acid for cell imaging. *Int. J. Nanomedicine* **2014**, *9*, 5071–5078, doi:10.2147/IJN.S68575.
20. Qu, S.; Wang, X.; Lu, Q.; Liu, X.; Wang, L. A Biocompatible Fluorescent Ink Based on Water-Soluble Luminescent Carbon Nanodots. *Angew. Chem. Int. Ed.* **2012**, *51*, 12215–12218, doi:10.1002/anie.201206791.
21. Liu, M.L.; Chen, B.B.; Li, C.M.; Huang, C.Z. Carbon dots: synthesis, formation mechanism, fluorescence origin and sensing applications. *Green Chem.* **2019**, *21*, 449–471, doi:10.1039/C8GC02736F.
22. Wei, W.; Xu, C.; Wu, L.; Wang, J.; Ren, J.; Qu, X. Non-Enzymatic-Browning-Reaction: A Versatile Route for Production of Nitrogen-Doped Carbon Dots with

- Tunable Multicolor Luminescent Display. *Sci. Rep.* **2014**, *4*, 3564, doi:10.1038/srep03564.
23. Ge, J.; Jia, Q.; Liu, W.; Guo, L.; Liu, Q.; Lan, M.; Zhang, H.; Meng, X.; Wang, P. Red-Emissive Carbon Dots for Fluorescent, Photoacoustic, and Thermal Theranostics in Living Mice. *Adv. Mater.* **2015**, *27*, 4169–4177, doi:10.1002/adma.201500323.
 24. Liu, J.-H.; Anilkumar, P.; Cao, L.; Wang, X.; Yang, S.-T.; Luo, P.G.; Wang, H.; Lu, F.; Mezziani, M.J.; Liu, Y.; et al. Cytotoxicity evaluations of fluorescent carbon nanoparticles. *Nano LIFE* **2010**, *01*, 153–161, doi:10.1142/S1793984410000158.
 25. Ray, S.C.; Saha, A.; Jana, N.R.; Sarkar, R. Fluorescent Carbon Nanoparticles: Synthesis, Characterization, and Bioimaging Application. *J. Phys. Chem. C* **2009**, *113*, 18546–18551, doi:10.1021/jp905912n.
 26. Ding, H.; Cheng, L.-W.; Ma, Y.-Y.; Kong, J.-L.; Xiong, H.-M. Luminescent carbon quantum dots and their application in cell imaging. *New J. Chem.* **2013**, *37*, 2515, doi:10.1039/c3nj00366c.
 27. Li, Q.; Ohulchanskyy, T.Y.; Liu, R.; Koynov, K.; Wu, D.; Best, A.; Kumar, R.; Bonoiu, A.; Prasad, P.N. Photoluminescent Carbon Dots as Biocompatible Nanoprobes for Targeting Cancer Cells in Vitro. *J. Phys. Chem. C* **2010**, *114*, 12062–12068, doi:10.1021/jp911539r.
 28. Yang, S.-T.; Cao, L.; Luo, P.G.; Lu, F.; Wang, X.; Wang, H.; Mezziani, M.J.; Liu, Y.; Qi, G.; Sun, Y.-P. Carbon Dots for Optical Imaging in vivo. *J. Am. Chem. Soc.* **2009**, *131*, 11308–11309, doi:10.1021/ja904843x.
 29. Li, H.; Zhang, Y.; Wang, L.; Tian, J.; Sun, X. Nucleic acid detection using carbon nanoparticles as a fluorescent sensing platform. *Chem. Commun. Camb. Engl.* **2011**, *47*, 961–963, doi:10.1039/c0cc04326e.
 30. Ma, N.; Jiang, W.; Li, T.; Zhang, Z.; Qi, H.; Yang, M. Fluorescence aggregation assay for the protein biomarker mucin 1 using carbon dot-labeled antibodies and aptamers. *Microchim. Acta* **2015**, *182*, 443–447, doi:10.1007/s00604-014-1386-3.
 31. Jing, Y.; Zhu, Y.; Yang, X.; Shen, J.; Li, C. Ultrasound-triggered smart drug release from multifunctional core-shell capsules one-step fabricated by coaxial electrospray

- method. *Langmuir ACS J. Surf. Colloids* **2011**, 27, 1175–1180, doi:10.1021/la1042734.
32. Tang, J.; Kong, B.; Wu, H.; Xu, M.; Wang, Y.; Wang, Y.; Zhao, D.; Zheng, G. Carbon nanodots featuring efficient FRET for real-time monitoring of drug delivery and two-photon imaging. *Adv. Mater. Deerfield Beach Fla* **2013**, 25, 6569–6574, doi:10.1002/adma.201303124.
 33. Zheng, M.; Liu, S.; Li, J.; Qu, D.; Zhao, H.; Guan, X.; Hu, X.; Xie, Z.; Jing, X.; Sun, Z. Integrating oxaliplatin with highly luminescent carbon dots: an unprecedented theranostic agent for personalized medicine. *Adv. Mater. Deerfield Beach Fla* **2014**, 26, 3554–3560, doi:10.1002/adma.201306192.
 34. Liu, C.; Zhang, P.; Zhai, X.; Tian, F.; Li, W.; Yang, J.; Liu, Y.; Wang, H.; Wang, W.; Liu, W. Nano-carrier for gene delivery and bioimaging based on carbon dots with PEI-passivation enhanced fluorescence. *Biomaterials* **2012**, 33, 3604–3613, doi:10.1016/j.biomaterials.2012.01.052.
 35. Li, H.; Luo, Y.; Sun, X. Fluorescence resonance energy transfer dye-labeled probe for fluorescence-enhanced DNA detection: An effective strategy to greatly improve discrimination ability toward single-base mismatch. *Biosens. Bioelectron.* **2011**, 27, 167–171, doi:10.1016/j.bios.2011.06.037.
 36. Greotti, E.; Capitanio, P.; Wong, A.; Pozzan, T.; Pizzo, P.; Pendin, D. Familial Alzheimer's disease-linked presenilin mutants and intracellular Ca²⁺ handling: A single-organelle, FRET-based analysis. *Cell Calcium* **2019**, 79, 44–56, doi:10.1016/j.ceca.2019.02.005.
 37. Solís, C.; Russell, B. CapZ integrates several signaling pathways in response to mechanical stiffness. *J. Gen. Physiol.* **2019**, 151, 660–669, doi:10.1085/jgp.201812199.
 38. Rosal, B. del; Benayas, A. Strategies to Overcome Autofluorescence in Nanoprobe-Driven In Vivo Fluorescence Imaging. *Small Methods* **2018**, 2, 1800075, doi:10.1002/smt.201800075.
 39. Mithöfer, A.; Mazars, C. Aequorin-based measurements of intracellular Ca²⁺-signatures in plant cells. *Biol. Proced. Online* **2002**, 4, 105–118, doi:10.1251/bpo40.

40. Lim, D.; Bertoli, A.; Sorgato, M.C.; Moccia, F. Generation and usage of aequorin lentiviral vectors for Ca(2+) measurement in sub-cellular compartments of hard-to-transfect cells. *Cell Calcium* **2016**, *59*, 228–239, doi:10.1016/j.ceca.2016.03.001.
41. Cobbold, P.H.; Cuthbertson, K.S.; Goyns, M.H.; Rice, V. Aequorin measurements of free calcium in single mammalian cells. *J. Cell Sci.* **1983**, *61*, 123–136.
42. Granatiero, V.; Patron, M.; Tosatto, A.; Merli, G.; Rizzuto, R. The use of aequorin and its variants for Ca²⁺ measurements. *Cold Spring Harb. Protoc.* **2014**, *2014*, 9–16, doi:10.1101/pdb.top066118.
43. Zeinoddini, M.; Khajeh, K.; Hosseinkhani, S.; Saeedinia, A.R.; Robatjazi, S.-M. Stabilisation of recombinant aequorin by polyols: activity, thermostability and limited proteolysis. *Appl. Biochem. Biotechnol.* **2013**, *170*, 273–280, doi:10.1007/s12010-013-0096-3.
44. Iwano, S.; Sugiyama, M.; Hama, H.; Watakabe, A.; Hasegawa, N.; Kuchimaru, T.; Tanaka, K.Z.; Takahashi, M.; Ishida, Y.; Hata, J.; et al. Single-cell bioluminescence imaging of deep tissue in freely moving animals. *Science* **2018**, *359*, 935–939, doi:10.1126/science.aag1067.
45. Waidmann, M.S.; Bleichrodt, F.S.; Laslo, T.; Riedel, C.U. Bacterial luciferase reporters: the Swiss army knife of molecular biology. *Bioeng. Bugs* **2011**, *2*, 8–16, doi:10.4161/bbug.2.1.13566.
46. Ke, D.; Tu, S.-C. Activities, kinetics and emission spectra of bacterial luciferase-fluorescent protein fusion enzymes. *Photochem. Photobiol.* **2011**, *87*, 1346–1353, doi:10.1111/j.1751-1097.2011.01001.x.
47. Cui, B.; Zhang, L.; Song, Y.; Wei, J.; Li, C.; Wang, T.; Wang, Y.; Zhao, T.; Shen, X. Engineering an Enhanced, Thermostable, Monomeric Bacterial Luciferase Gene As a Reporter in Plant Protoplasts. *PLOS ONE* **2014**, *9*, e107885, doi:10.1371/journal.pone.0107885.
48. Hollis, R.P.; Lagido, C.; Pettitt, J.; Porter, A.J.R.; Killham, K.; Paton, G.I.; Glover, L.A. Toxicity of the bacterial luciferase substrate, n-decyl aldehyde, to *Saccharomyces cerevisiae* and *Caenorhabditis elegans*. *FEBS Lett.* **2001**, *506*, 140–142, doi:10.1016/S0014-5793(01)02905-2.

49. Coleman, S.M.; McGregor, A. A bright future for bioluminescent imaging in viral research. *Future Virol.* **2015**, *10*, 169–183, doi:10.2217/fvl.14.96.
50. de Wet, J.R.; Wood, K.V.; DeLuca, M.; Helinski, D.R.; Subramani, S. Firefly luciferase gene: structure and expression in mammalian cells. *Mol. Cell. Biol.* **1987**, *7*, 725–737, doi:10.1128/mcb.7.2.725.
51. Branchini, B.R.; Southworth, T.L.; Fontaine, D.M.; Kohrt, D.; Welcome, F.S.; Florentine, C.M.; Henricks, E.R.; DeBartolo, D.B.; Michelini, E.; Cevenini, L.; et al. Red-emitting chimeric firefly luciferase for in vivo imaging in low ATP cellular environments. *Anal. Biochem.* **2017**, *534*, 36–39, doi:10.1016/j.ab.2017.07.001.
52. Gibbons, A.E.; Luker, K.E.; Luker, G.D. Dual Reporter Bioluminescence Imaging with NanoLuc and Firefly Luciferase BT - Reporter Gene Imaging: Methods and Protocols. In; Dubey, P., Ed.; Springer New York: New York, NY, 2018; pp. 41–50 ISBN 978-1-4939-7860-1.
53. Paulmurugan, R.; Gambhir, S.S. Monitoring Protein–Protein Interactions Using Split Synthetic Renilla Luciferase Protein-Fragment-Assisted Complementation. *Anal. Chem.* **2003**, *75*, 1584–1589, doi:10.1021/ac020731c.
54. Bhaumik, S.; Gambhir, S.S. Optical imaging of Renilla luciferase reporter gene expression in living mice. *Proc. Natl. Acad. Sci.* **2002**, *99*, 377–382, doi:10.1073/pnas.012611099.
55. Tannous, B.A.; Kim, D.-E.; Fernandez, J.L.; Weissleder, R.; Breakefield, X.O. Codon-Optimized Gaussia Luciferase cDNA for Mammalian Gene Expression in Culture and in Vivo. *Mol. Ther.* **2005**, *11*, 435–443, doi:10.1016/j.ymthe.2004.10.016.
56. Degeling, M.H.; Bovenberg, M.S.S.; Lewandrowski, G.K.; de Gooijer, M.C.; Vleggeert-Lankamp, C.L.A.; Tannous, M.; Maguire, C.A.; Tannous, B.A. Directed Molecular Evolution Reveals Gaussia Luciferase Variants with Enhanced Light Output Stability. *Anal. Chem.* **2013**, *85*, 3006–3012, doi:10.1021/ac4003134.
57. Hunt, E.A.; Moutsipoulou, A.; Broyles, D.; Head, T.; Dikici, E.; Daunert, S.; Deo, S.K. Expression of a soluble truncated Vargula luciferase in Escherichia coli. *Protein Expr. Purif.* **2017**, *132*, 68–74, doi:10.1016/j.pep.2017.01.007.

58. Thompson, E.M.; Nagata, S.; Tsuji, F.I. Vargula hilgendorffii luciferase: a secreted reporter enzyme for monitoring gene expression in mammalian cells. *Gene* **1990**, *96*, 257–262, doi:10.1016/0378-1119(90)90261-O.
59. Ereemeeva, E.V.; Markova, S.V.; Vysotski, E.S. Highly active BRET-reporter based on yellow mutant of Renilla muelleri luciferase. *Dokl. Biochem. Biophys.* **2013**, *450*, 147–150, doi:10.1134/S1607672913030095.
60. Markova, S.V.; Golz, S.; Frank, L.A.; Kalthof, B.; Vysotski, E.S. Cloning and Expression of cDNA for a Luciferase from the Marine Copepod Metridia longa A NOVEL SECRETED BIOLUMINESCENT REPORTER ENZYME. *J. Biol. Chem.* **2004**, *279*, 3212–3217, doi:10.1074/jbc.M309639200.
61. Song, G.; Wu, Q.-P.; Xu, T.; Liu, Y.-L.; Xu, Z.-G.; Zhang, S.-F.; Guo, Z.-Y. Quick preparation of nanoluciferase-based tracers for novel bioluminescent receptor-binding assays of protein hormones: Using erythropoietin as a model. *J. Photochem. Photobiol. B* **2015**, *153*, 311–316, doi:10.1016/j.jphotobiol.2015.10.014.
62. He, S.-X.; Song, G.; Shi, J.-P.; Guo, Y.-Q.; Guo, Z.-Y. Nanoluciferase as a novel quantitative protein fusion tag: Application for overexpression and bioluminescent receptor-binding assays of human leukemia inhibitory factor. *Biochimie* **2014**, *106*, 140–148, doi:10.1016/j.biochi.2014.08.012.
63. Abbott, N.J.; Rönnbäck, L.; Hansson, E. Astrocyte–endothelial interactions at the blood–brain barrier. *Nat. Rev. Neurosci.* **2006**, *7*, 41–53, doi:10.1038/nrn1824.
64. Abbott, N.J.; Patabendige, A.A.K.; Dolman, D.E.M.; Yusof, S.R.; Begley, D.J. Structure and function of the blood–brain barrier. *Neurobiol. Dis.* **2010**, *37*, 13–25, doi:10.1016/j.nbd.2009.07.030.
65. Grabrucker, A.M.; Ruozi, B.; Belletti, D.; Pederzoli, F.; Forni, F.; Vandelli, M.A.; Tosi, G. Nanoparticle transport across the blood brain barrier. *Tissue Barriers* **2016**, *4*, doi:10.1080/21688370.2016.1153568.
66. Pardridge, W.M. The Blood-Brain Barrier: Bottleneck in Brain Drug Development. **2005**, *2*, 12.
67. Wohlfart, S.; Gelperina, S.; Kreuter, J. Transport of drugs across the blood–brain barrier by nanoparticles. *J. Controlled Release* **2012**, *161*, 264–273, doi:10.1016/j.jconrel.2011.08.017.

68. Md, S.; Mustafa, G.; Baboota, S.; Ali, J. Nanoneurotherapeutics approach intended for direct nose to brain delivery. *Drug Dev. Ind. Pharm.* **2015**, *41*, 1922–1934, doi:10.3109/03639045.2015.1052081.
69. Campbell, M.; Humphries, P. The Blood-Retina Barrier. In *Biology and Regulation of Blood-Tissue Barriers*; Cheng, C.Y., Ed.; Advances in Experimental Medicine and Biology; Springer: New York, NY, 2013; pp. 70–84 ISBN 978-1-4614-4711-5.
70. Schlosshauer, B.; Steuer, H. Comparative Anatomy, Physiology and In Vitro Models of the Blood-Brain and Blood-Retina Barrier. *Curr. Med. Chem. - Cent. Nerv. Syst. Agents* **2002**, *2*, 175–186, doi:10.2174/1568015023357978.
71. Steuer, H.; Jaworski, A.; Elger, B.; Kaussmann, M.; Keldenich, J.; Schneider, H.; Stoll, D.; Schlosshauer, B. Functional Characterization and Comparison of the Outer Blood–Retina Barrier and the Blood–Brain Barrier. *Invest. Ophthalmol. Vis. Sci.* **2005**, *46*, 1047–1053, doi:10.1167/iovs.04-0925.
72. Zheng, P.-P.; Romme, E.; van der Spek, P.J.; Dirven, C.M.F.; Willemsen, R.; Kros, J.M. Glut1/SLC2A1 is crucial for the development of the blood-brain barrier in vivo. *Ann. Neurol.* **2010**, *68*, 835–844, doi:10.1002/ana.22318.
73. Peura, L.; Malmioja, K.; Huttunen, K.; Leppänen, J.; Hämäläinen, M.; Forsberg, M.M.; Gynther, M.; Rautio, J.; Laine, K. Design, synthesis and brain uptake of LAT1-targeted amino acid prodrugs of dopamine. *Pharm. Res.* **2013**, *30*, 2523–2537.
74. Kato, S.; Itoh, K.; Yaoi, T.; Tozawa, T.; Yoshikawa, Y.; Yasui, H.; Kanamura, N.; Hoshino, A.; Manabe, N.; Yamamoto, K.; et al. Organ distribution of quantum dots after intraperitoneal administration, with special reference to area-specific distribution in the brain. *Nanotechnology* **2010**, *21*, 335103, doi:10.1088/0957-4484/21/33/335103.
75. Liu, D.; Lin, B.; Shao, W.; Zhu, Z.; Ji, T.; Yang, C. In Vitro and in Vivo Studies on the Transport of PEGylated Silica Nanoparticles across the Blood–Brain Barrier. *ACS Appl. Mater. Interfaces* **2014**, *6*, 2131–2136, doi:10.1021/am405219u.
76. Sonavane, G.; Tomoda, K.; Makino, K. Biodistribution of colloidal gold nanoparticles after intravenous administration: effect of particle size. *Colloids Surf. B Biointerfaces* **2008**, *66*, 274–280, doi:10.1016/j.colsurfb.2008.07.004.

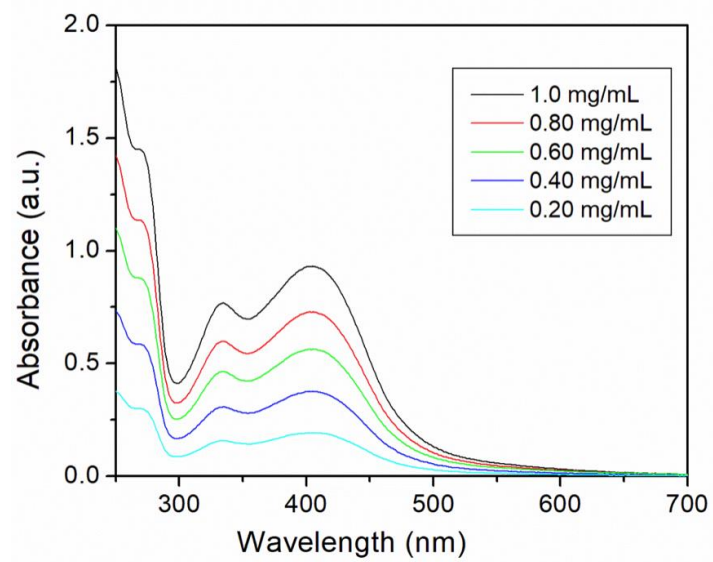
77. Huang, N.; Cheng, S.; Zhang, X.; Tian, Q.; Pi, J.; Tang, J.; Huang, Q.; Wang, F.; Chen, J.; Xie, Z.; et al. Efficacy of NGR peptide-modified PEGylated quantum dots for crossing the blood–brain barrier and targeted fluorescence imaging of glioma and tumor vasculature. *Nanomedicine Nanotechnol. Biol. Med.* **2017**, *13*, 83–93, doi:10.1016/j.nano.2016.08.029.
78. Tsuji, A.; Tamai, I. Carrier-mediated or specialized transport of drugs across the blood–brain barrier. *Adv. Drug Deliv. Rev.* **1999**, *36*, 277–290, doi:10.1016/S0169-409X(98)00084-2.
79. Hervé, F.; Ghinea, N.; Scherrmann, J.-M. CNS Delivery Via Adsorptive Transcytosis. *AAPS J.* **2008**, *10*, 455–472, doi:10.1208/s12248-008-9055-2.
80. Monsalve, Y.; Tosi, G.; Ruozi, B.; Belletti, D.; Vilella, A.; Zoli, M.; Vandelli, M.A.; Forni, F.; López, B.L.; Sierra, L. PEG-g-chitosan nanoparticles functionalized with the monoclonal antibody OX26 for brain drug targeting. *Nanomed.* **2015**, *10*, 1735–1750, doi:10.2217/nnm.15.29.
81. Kim, J.-Y.; Choi, W.I.; Kim, Y.H.; Tae, G. Brain-targeted delivery of protein using chitosan- and RVG peptide-conjugated, pluronic-based nano-carrier. *Biomaterials* **2013**, *34*, 1170–1178, doi:10.1016/j.biomaterials.2012.09.047.
82. Janaszewska, A.; Ziemba, B.; Ciepluch, K.; Appelhans, D.; Voit, B.; Klajnert, B.; Bryszewska, M. The biodistribution of maltotriose modified poly(propylene imine) (PPI) dendrimers conjugated with fluorescein—proofs of crossing blood–brain–barrier. *New J Chem* **2012**, *36*, 350–353, doi:10.1039/C1NJ20444K.
83. Park, T.-E.; Singh, B.; Li, H.; Lee, J.-Y.; Kang, S.-K.; Choi, Y.-J.; Cho, C.-S. Enhanced BBB permeability of osmotically active poly(mannitol-co-PEI) modified with rabies virus glycoprotein via selective stimulation of caveolar endocytosis for RNAi therapeutics in Alzheimer's disease. *Biomaterials* **2015**, *38*, 61–71, doi:10.1016/j.biomaterials.2014.10.068.
84. Dombu, C.Y.; Kroubi, M.; Zibouche, R.; Matran, R.; Betbeder, D. Characterization of endocytosis and exocytosis of cationic nanoparticles in airway epithelium cells. *Nanotechnology* **2010**, *21*, 355102, doi:10.1088/0957-4484/21/35/355102.
85. Agarwal, A.; Majumder, S.; Agrawal, H.; Majumdar, S.; P. Agrawal, G. Cationized Albumin Conjugated Solid Lipid Nanoparticles as Vectors for Brain Delivery of an

- Anti-Cancer Drug. *Curr. Nanosci.* **2011**, *7*, 71–80, doi:10.2174/157341311794480291.
86. Lin, T.; Zhao, P.; Jiang, Y.; Tang, Y.; Jin, H.; Pan, Z.; He, H.; Yang, V.C.; Huang, Y. Blood–Brain-Barrier-Penetrating Albumin Nanoparticles for Biomimetic Drug Delivery via Albumin-Binding Protein Pathways for Antiglioma Therapy. *ACS Nano* **2016**, *10*, 9999–10012, doi:10.1021/acsnano.6b04268.
 87. Gan, C.W.; Feng, S.-S. Transferrin-conjugated nanoparticles of Poly(lactide)-d- α -Tocopheryl polyethylene glycol succinate diblock copolymer for targeted drug delivery across the blood–brain barrier. *Biomaterials* **2010**, *31*, 7748–7757, doi:10.1016/j.biomaterials.2010.06.053.
 88. Ulbrich, K.; Hekmatara, T.; Herbert, E.; Kreuter, J. Transferrin- and transferrin-receptor-antibody-modified nanoparticles enable drug delivery across the blood–brain barrier (BBB). *Eur. J. Pharm. Biopharm.* **2009**, *71*, 251–256, doi:10.1016/j.ejpb.2008.08.021.
 89. Visser, C.C.; Stevanović, S.; Voorwinden, L.H.; Bloois, van L.; Gaillard, P.J.; Danhof, M.; Crommelin, D.J.A.; Boer, de A.G. Targeting liposomes with protein drugs to the blood–brain barrier in vitro. *Eur. J. Pharm. Sci.* **2005**, *25*, 299–305, doi:10.1016/j.ejps.2005.03.008.
 90. Fornaguera, C.; Dols-Perez, A.; Calderó, G.; García-Celma, M.J.; Camarasa, J.; Solans, C. PLGA nanoparticles prepared by nano-emulsion templating using low-energy methods as efficient nanocarriers for drug delivery across the blood–brain barrier. *J. Controlled Release* **2015**, *211*, 134–143, doi:10.1016/j.jconrel.2015.06.002.
 91. Sélo, I.; Négroni, L.; Créminon, C.; Grassi, J.; Wal, J.M. Preferential labeling of alpha-amino N-terminal groups in peptides by biotin: application to the detection of specific anti-peptide antibodies by enzyme immunoassays. *J. Immunol. Methods* **1996**, *199*, 127–138.
 92. Woo, J.; Howell, M.H.; von Arnim, A.G. Structure-function studies on the active site of the coelenterazine-dependent luciferase from *Renilla*. *Protein Sci.* **2008**, *17*, 725–735, doi:10.1110/ps.073355508.

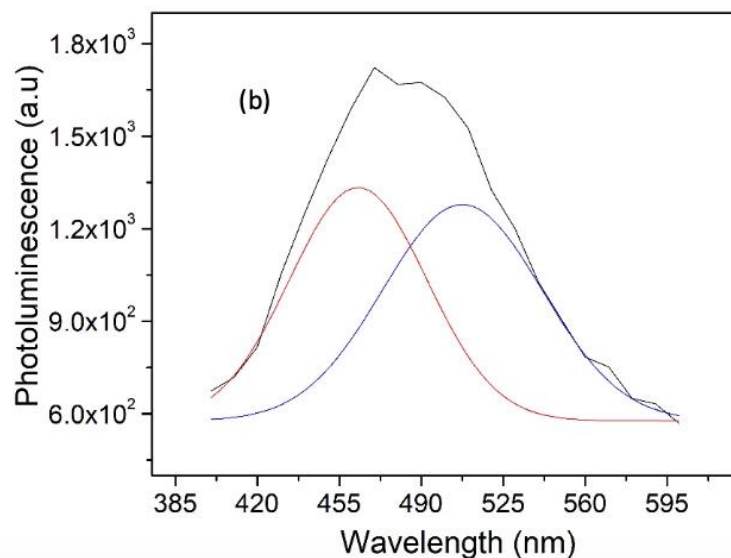
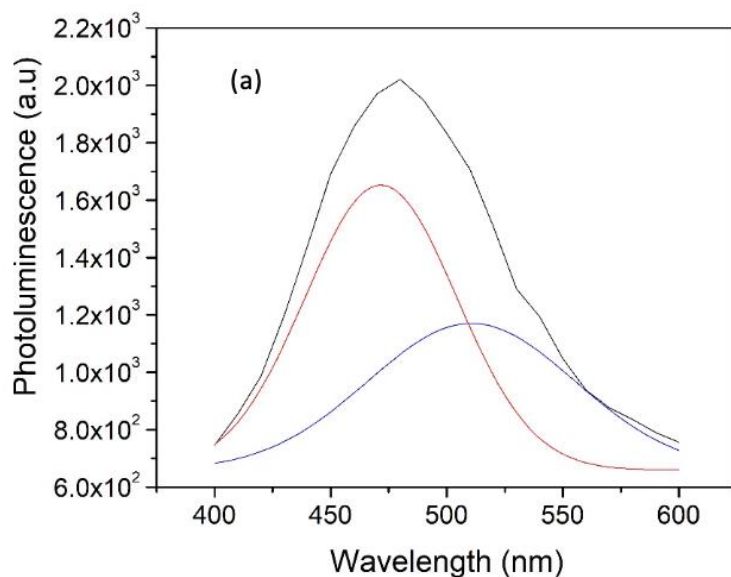
93. Ishida, N.; Kawakita, M. Molecular physiology and pathology of the nucleotide sugar transporter family (SLC35). *Pflüg. Arch.* **2004**, *447*, 768–775, doi:10.1007/s00424-003-1093-0.
94. Percherancier, Y.; Berchiche, Y.A.; Slight, I.; Volkmer-Engert, R.; Tamamura, H.; Fujii, N.; Bouvier, M.; Heveker, N. Bioluminescence Resonance Energy Transfer Reveals Ligand-induced Conformational Changes in CXCR4 Homo- and Heterodimers. *J. Biol. Chem.* **2005**, *280*, 9895–9903, doi:10.1074/jbc.M411151200.
95. Marullo, S.; Bouvier, M. Resonance energy transfer approaches in molecular pharmacology and beyond. *Trends Pharmacol. Sci.* **2007**, *28*, 362–365, doi:10.1016/j.tips.2007.06.007.
96. Pitkänen, L.; Pelkonen, J.; Ruponen, M.; Rönkkö, S.; Urtti, A. Neural retina limits the nonviral gene transfer to retinal pigment epithelium in an in vitro bovine eye model. *AAPS J.* **2004**, *6*, 72–80, doi:10.1208/aapsj060325.
97. Huang, D.; Chen, Y.-S.; Thakur, S.S.; Rupenthal, I.D. Ultrasound-mediated nanoparticle delivery across ex vivo bovine retina after intravitreal injection. *Eur. J. Pharm. Biopharm.* **2017**, *119*, 125–136, doi:10.1016/j.ejpb.2017.06.009.

Appendices

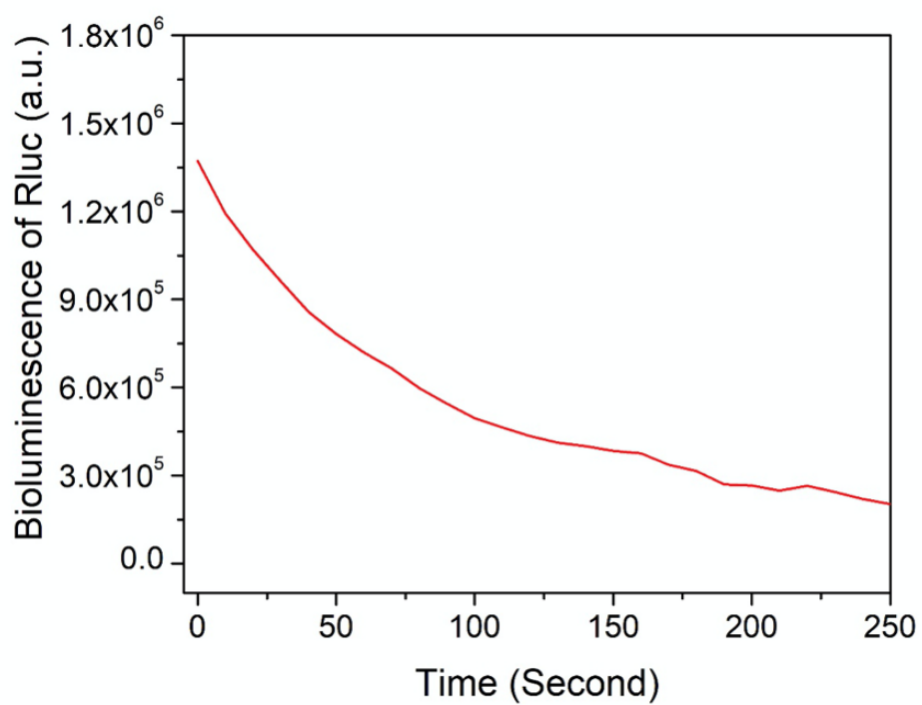
Appendix 1: UV-vis absorption spectrum of different concentrations of CDs.



Appendix 2: (a) BRET spectrum of sample made through EDC-mediated conjugation of 0.40 mg/mL CD and 2 μ M Rluc for 6.5 hours. (b) BRET spectrum of sample made through EDC-mediated conjugation of 0.80 mg/mL CD and 2 μ M Rluc for 6.5 hours. The black line represents the BRET profile of the sample; the red line and the blue line were obtained using multi-peak fitting and represent bioluminescence of Rluc and photoluminescence of CD respectively.



Appendix 3: Bioluminescence of Rluc as a function of time after introduction of CTZ



Curriculum Vitae

Name: Jisu Song

Post-secondary Education and Degrees: The University of Western Ontario
London, Ontario, Canada
2013-2018 B.M.Sc. Honours

The University of Western Ontario
London, Ontario, Canada
2018-2020 M.E.Sc.

Honours and Awards: Western Graduate Research Scholarship
2018-2019, 2019-2020

Related Work Experience Teaching Assistant
the University of Western Ontario
2018-2020

Publications:

Hwang, E., **Song, J.** & Zhang, J. Integration of Nanomaterials and Bioluminescence Resonance Energy Transfer Techniques for Sensing Biomolecules. *Biosensors*. 9, E42 (2019).

Song, J. & Zhang, J. Self-illumination of Carbon Dots by Bioluminescence Resonance Energy Transfer. *Scientific Reports*. 9, 13796 (2019).